

Exhibit HH

Exhibit E-6

Invalidity of U.S. Patent No. 7,725,253 (“’253 Patent”) under Pre-AIA Section 102 or Section 103 in view of Welch et al., “High-Performance Wide-Area Optical Tracking: The HiBall Tracking System,” PRESENCE, Vol. 10, No. 1, February 2001 (“Welch 2001”)¹

Welch 2001 was published in February 2001. Plaintiffs belatedly asserted a priority date of June 13, 2001 for the ’253 Patent on December 22, 2021, 71 days after the Court’s deadline. Defendants have reviewed Plaintiffs’ alleged evidence of the purported June 13, 2001 priority date, and maintain that the ’253 Patent is not entitled to this priority date. *See* Defendants’ March 15, 2022 Supplemental Invalidity Contentions. Defendants reserve their objections to Plaintiffs’ belated assertion of the new priority date and expressly reserve all rights to challenge this alleged new priority date. As such, Defendants assume for the sake of these invalidity contentions, that the priority date for the ’253 Patent is August 9, 2002 based on the first filed Provisional Application from which the ’253 Patent claims priority. (Defendants do not concede nor agree that Plaintiffs are even entitled to this date.) Assuming this priority date, Welch 2001 qualifies as prior art under at least pre-AIA Sections 102(a) and (b) to the ’253 Patent.

As described herein, the asserted claims of the ’253 Patent are invalid (a) under one or more sections of 35 U.S.C. § 102 as anticipated expressly or inherently by Welch 2001 (including the documents incorporated into Welch 2001 by reference), and (b) under 35 U.S.C. § 103 as obvious in view of Welch 2001 standing alone and, additionally, in combination with the knowledge of one of ordinary skill in the art, and/or other prior art, including but not limited to the prior art identified in Defendants’ Invalidity Contentions and the prior art described in the claim charts attached in Exhibits E-1 – E-23. With respect to the proposed modifications to Welch 2001, as of the priority date of the ’253 Patent, such modification would have been obvious to try, an obvious combination of prior art elements according to known methods to yield predictable results, a simple substitution of one known element for another to obtain predictable results, a use of known techniques to improve a similar device or method in the same way, an application of a known technique to a known device or method ready for improvement to yield predictable results, a variation of a known work in one field of endeavor for use in either the same field or a different one based on design incentives or other market forces with variations that are predictable to one of ordinary skill in the art, and/or obvious in view of teachings, suggestions, and motivations in the prior art that would have led one of ordinary skill to modify or combine the prior art references.

¹ Discovery in this case is ongoing and, accordingly, this invalidity chart is not to be considered final. Defendants have conducted the invalidity analysis herein without having fully undergone claim construction and a *Markman* hearing. By charting the prior art against the claim(s) herein, Defendants are not admitting nor agreeing to Plaintiffs’ interpretation of the claims at issue in this case. Additionally, these charts provide representative examples of portions of the charted references that disclose the indicated limitations under Plaintiffs’ application of the claims; additional portions of these references other than the representative examples provided herein may also disclose the indicated limitation(s) and Defendants contend that the asserted claim(s) are invalid in light of the charted reference(s) as a whole. Defendants reserve the right to rely on additional citations or sources of evidence that also may be applicable, or that may become applicable in light of claim construction, changes in Plaintiffs’ infringement contentions, and/or information obtained during discovery as the case progresses. Further, by submitting these invalidity contentions, Defendants do not waive and hereby expressly reserve their right to raise other invalidity defenses, including but not limited to defenses under Sections 101 and 112. Defendants reserve the right to amend or supplement this claim chart at a later date, including after the Court’s order construing disputed claim terms.

Exhibit E-6

All cross-references should be understood to include material that is cross-referenced within the cross-reference. Where a particular figure is cited, the citation should be understood to encompass the caption and description of the figure as well as any text relating to or describing the figure. Conversely, where particular text referring to a figure is cited, the citation should be understood to include the figure as well.

A. INDEPENDENT CLAIM 1

CLAIM 1	Welch 2001
[1.pre] A tracking system comprising:	<p>At least under Plaintiffs' apparent infringement theory, Welch 2001 discloses, either expressly or inherently, a tracking system and method for tracking an object.</p> <p>No party has yet asserted that the preamble is limiting, nor has the Court construed the preamble as limiting. However, to the extent that the preamble is limiting, it is disclosed by Welch 2001.</p> <p>In the alternative, this element would be obvious over Welch 2001 in light of the other references disclosed in Defendants' Invalidity Contentions and/or the knowledge of one of ordinary skill in the art.</p> <p><i>See, e.g.:</i></p>

Exhibit E-6

CLAIM 1	Welch 2001
	<div data-bbox="525 243 1638 779"> <p>Initial wide-area opto-electronic idea</p> <p>Simpler LED panels and off-line calibration</p> <p>SCAAT and autocalibration</p> <p>1984 1991 1993 1995 1997 1999</p> <p>Bishop's VLSI Self-Tracker</p> <p>Original system (SIGGRAPH 91)</p> <p>The HiBall</p> <p>The HiBall system</p> </div> <p>Figure 1.</p> <p>We present results and a complete description of our most recent electro-optical system, the HiBall Tracking System. In particular, we discuss motivation for the geometric configuration and describe the novel optical, mechanical, electronic, and algorithmic aspects that enable unprecedented speed, resolution, accuracy, robustness, and flexibility. Welch 2001 at Abstract.</p> <p>Systems for head tracking for interactive computer graphics have been explored for more than thirty years. Welch 2001 at Section 1.</p> <p>As part of his 1984 dissertation on Self-Tracker, Bishop put forward the idea of outward-looking tracking systems based on user-mounted sensors that estimate user pose by observing landmarks in the environment (Bishop, 1984). He described two kinds of landmarks: high signal-to-noise-ratio beacons such as light-emitting diodes (LEDs) and low signal-to-noise-ratio landmarks such as naturally occurring features. Bishop designed and demonstrated custom VLSI chips (figure 2) that combined image sensing and processing on a single chip (Bishop & Fuchs, 1984). The idea was to combine multiple instances of these chips into an outward-looking cluster that estimated cluster motion by observing natural features in the unmodified environment. Integrating the resulting</p>

Exhibit E-6

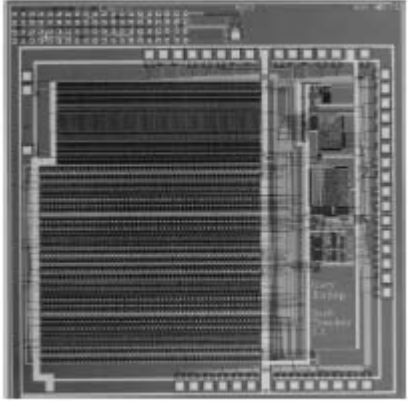
CLAIM 1	Welch 2001
	<p data-bbox="499 240 1969 344">motion to estimate pose is prone to accumulating error, so further development required a complementary system based on easily detectable landmarks (LEDs) at known locations. Welch 2001 at Section 1.2.</p> <div data-bbox="506 381 947 865">  <p data-bbox="527 816 646 849">Figure 2.</p> </div> <p data-bbox="499 906 1915 1198">In 1991, we demonstrated a working, scalable, electro-optical head-tracking system in the Tomorrow's Realities gallery at that year's ACM SIGGRAPH conference (Wang et al., 1990; Wang, Chi, & Fuchs, 1990; Ward et al., 1992). The system (figure 3) used four, head-worn, lateral-effect photodiodes that looked upward at a regular array of infrared LEDs installed in precisely machined ceiling panels. A user-worn backpack contained electronics that digitized and communicated the photo-coordinates of the sighted LEDs. Photogrammetric techniques were used to compute a user's head pose using the known LED positions and the corresponding measured photo-coordinates from each LEPD sensor (Azuma & Ward, 1991).</p> <p data-bbox="499 1198 848 1230">Welch 2001 at Section 1.2.</p>

Exhibit E-6


CLAIM 1	Welch 2001
	

Exhibit E-6

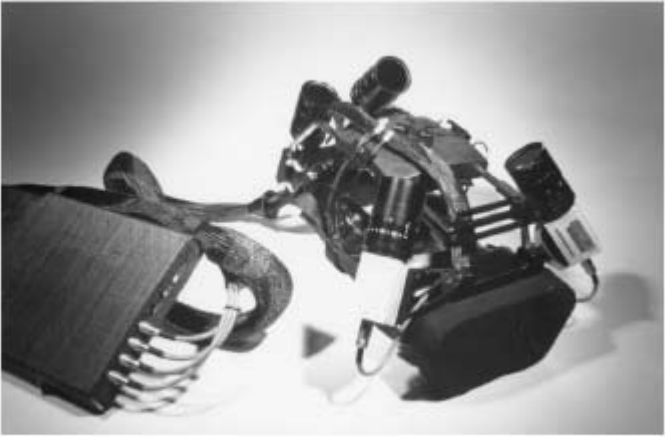
CLAIM 1	Welch 2001
	<div data-bbox="506 240 1243 755"><p data-bbox="512 711 625 738">Figure 3.</p></div>

Exhibit E-6



CLAIM 1	Welch 2001
	<div data-bbox="508 245 1045 662">  </div> <div data-bbox="569 695 978 1102">  </div> <div data-bbox="508 1122 630 1154"> <p>Figure 4.</p> </div> <p data-bbox="499 1203 1969 1419">In this article, we describe a new and vastly improved version of the 1991 system. We call the new system the HiBall Tracking System. Thanks to significant improvements in hardware and software, this HiBall system offers unprecedented speed, resolution, accuracy, robustness, and flexibility. The bulky and heavy sensors and backpack of the previous system have been replaced by a small HiBall unit (figure 4, bottom). In addition, the precisely machined LED ceiling panels of the previous system have been replaced by looser-tolerance panels that are relatively inexpensive to make and simple to install (figure 4, top; figure 10). Finally, we are using an unusual</p>

Exhibit E-6

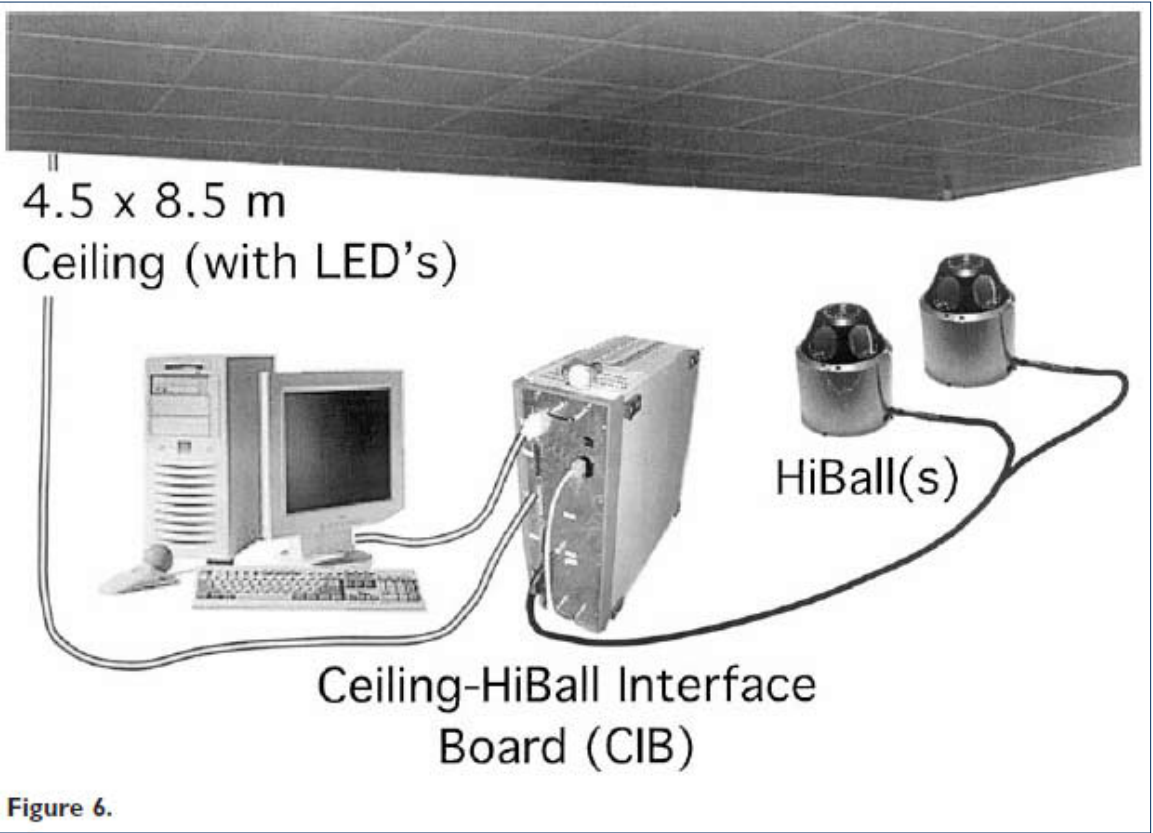
CLAIM 1	Welch 2001
	<p data-bbox="499 240 1969 311">Kalman-filter-based algorithm that generates very accurate pose estimates at a high rate with low latency, and that simultaneously self-calibrates the system.</p> <p data-bbox="499 344 844 376">Welch 2001 at Section 1.3.</p> <div data-bbox="508 412 1654 1240"><p data-bbox="529 587 961 701">4.5 x 8.5 m Ceiling (with LED's)</p><p data-bbox="1276 863 1465 912">HiBall(s)</p><p data-bbox="823 1068 1318 1182">Ceiling-HiBall Interface Board (CIB)</p><p data-bbox="508 1205 625 1230">Figure 6.</p></div> <p data-bbox="499 1279 1348 1312"><i>See also</i> Defendants' Invalidity Contentions for further discussion.</p>

Exhibit E-6

CLAIM 1	Welch 2001
[1.a] an estimation subsystem; and	<p>At least under Plaintiffs' apparent infringement theory, Welch 2001 discloses, either expressly or inherently, an estimation subsystem. In the alternative, this element would be obvious over Welch 2001 in light of the other references disclosed in Defendants' Invalidity Contentions and/or the knowledge of one of ordinary skill in the art.</p> <p><i>See, e.g.:</i></p> <p>Systems for head tracking for interactive computer graphics have been explored for more than thirty years (Sutherland, 1968). As illustrated in figure 1, the authors have been working on the problem for more than twenty years (Azuma, 1993, 1995; Azuma & Bishop, 1994a, 1994b; Azuma & Ward, 1991; Bishop, 1984; Gottschalk & Hughes, 1993; UNC Tracker Project, 2000; Wang, 1990; Wang et al., 1990; Ward, Azuma, Bennett, Gottschalk, & Fuchs, 1992; Welch, 1995, 1996; Welch & Bishop, 1997; Welch et al., 1999). From the beginning, our efforts have been targeted at wide-area applications in particular. This focus was originally motivated by applications for which we believed that actually walking around the environment would be superior to virtually "flying." For example, we wanted to interact with room-filling virtual molecular models, and to naturally explore life-sized virtual architectural models. Today, we believe that a wide-area system with high performance everywhere in our laboratory provides increased flexibility for all of our graphics, vision, and interaction research.</p> <p>Welch 2001 at Section 1.</p> <p>Thanks to significant improvements in hardware and software, this HiBall system offers unprecedented speed, resolution, accuracy, robustness, and flexibility. The bulky and heavy sensors and backpack of the previous system have been replaced by a small HiBall unit (figure 4, bottom). In addition, the precisely machined LED ceiling panels of the previous system have been replaced by looser-tolerance panels that are relatively inexpensive to make and simple to install (figure 4, top; figure 10). Finally, we are using an unusual Kalman-filter-based algorithm that generates very accurate pose estimates at a high rate with low latency, and that simultaneously self-calibrates the system.</p> <p>Welch 2001 at Section 1.3.</p>

Exhibit E-6



CLAIM 1	Welch 2001
	<div data-bbox="508 245 1045 662">  </div> <div data-bbox="569 696 976 1104">  </div> <div data-bbox="508 1122 630 1154"> <p>Figure 4.</p> </div> <p data-bbox="499 1203 1963 1344">During the design of the HiBall system, we made substantial use of simulation, in some domains to a very detailed level. For example, Zemax (Focus Software, 1995) was used extensively in the design and optimization of the optical design, including the design of the filter glass lenses, and geometry of the optical-component layout. Welch 2001 at Section 6.2.</p> <p data-bbox="499 1382 1963 1451">The HiBall Tracking System consists of three main components (figure 6). An outward-looking sensing unit we call the HiBall is fixed to each user to be tracked. The HiBall unit observes a subsystem of fixed-location</p>

Exhibit E-6

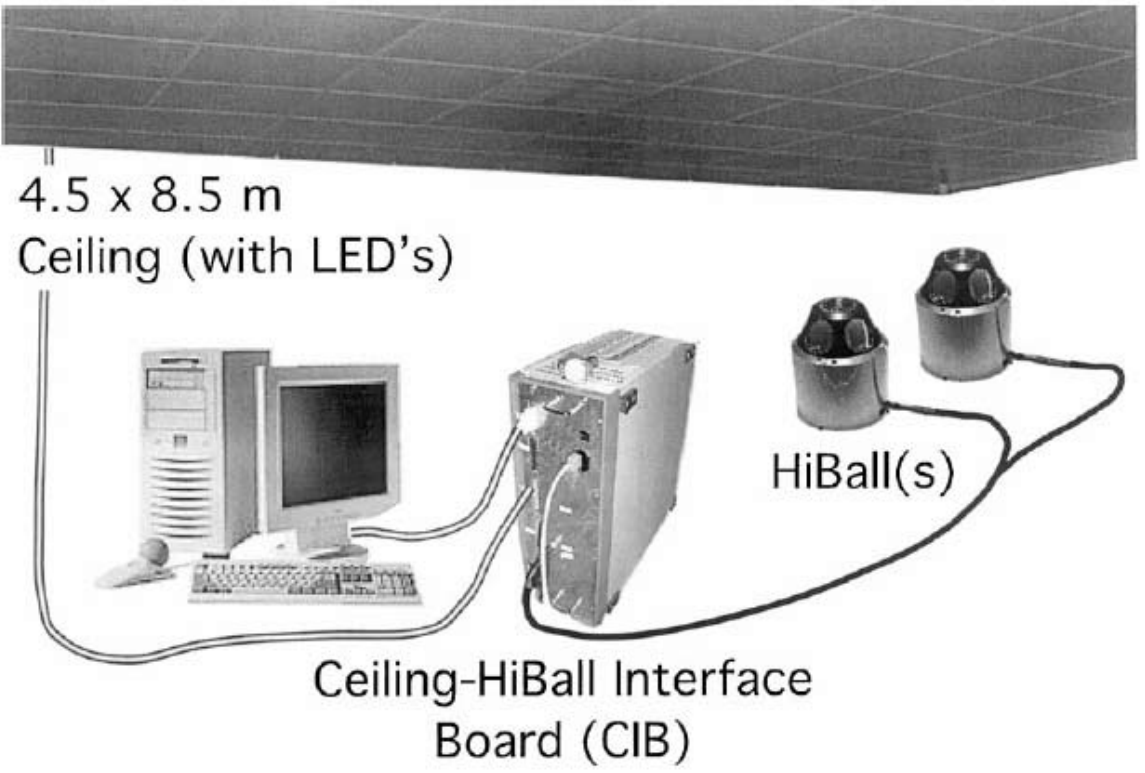
CLAIM 1	Welch 2001
	<p data-bbox="499 240 1913 310">infrared LEDs we call the Ceiling. Communication and synchronization between the host computer and these subsystems is coordinated by the Ceiling-HiBall Interface Board (CIB).</p> <p data-bbox="499 315 821 342">Welch 2001 at Section 3.</p> <div data-bbox="499 380 1650 1208">  <p data-bbox="527 553 961 667">4.5 x 8.5 m Ceiling (with LED's)</p> <p data-bbox="1276 829 1461 878">HiBall(s)</p> <p data-bbox="821 1040 1318 1149">Ceiling-HiBall Interface Board (CIB)</p> <p data-bbox="512 1170 621 1198">Figure 6.</p> </div> <p data-bbox="499 1252 1969 1425">This multiple constraint method had several drawbacks. First, it had a significantly lower estimate rate due to the need to collect multiple measurements per estimate. Second, the system of nonlinear equations did not account for the fact that the sensor fixture continued to move throughout the collection of the sequence of measurements. Instead, the method effectively assumes that the measurements were taken simultaneously. The violation of this simultaneity assumption could introduce significant error during even moderate motion. Finally, the method</p>

Exhibit E-6

CLAIM 1	Welch 2001
	<p>provided no means to identify or handle unusually noisy individual measurements. Thus, a single erroneous measurement could cause an estimate to jump away from an otherwise smooth track.</p> <p>Welch 2001 at Section 5.3.</p> <p>Once a particular view and LED have been chosen in this fashion, the CIB (section 4.3) is instructed to flash the LED and take a measurement as described in section 5.2. This single measurement is compared with a prediction obtained using equation (3), and the difference (or residual) is used to update the filter state and covariance matrices using the Kalman gain matrix. The Kalman gain is computed as a combination of the current filter covariance, the measurement noise variance (section 6.2.1), and the Jacobian of the measurement model. This recursive prediction-correction cycle continues in an ongoing fashion, a single constraint at a time.</p> <p>Welch 2001 at Section 5.3.</p> <p>The online measurements (section 5.2) are used to estimate the pose of the HiBall during operation. The 1991 system collected a group of diverse measurements for a variety of LEDs and sensors, and then used a method of simultaneous nonlinear equations called collinearity (Azuma & Ward, 1991) to estimate the pose of the sensor fixture shown in figure 3 (bottom).</p> <p>Welch 2001 at Section 5.3.</p> <p>In contrast, the approach we use with the new HiBall system produces tracker reports as each new measurement is made, rather than waiting to form a complete collection of observations. Because single measurements under constrain the mathematical solution, we refer to the approach as single-constraint-at-a-time (SCAAT) tracking (Welch, 1996; Welch & Bishop, 1997). The key is that the single measurements provide some information about the HiBall's state, and thus can be used to incrementally improve a previous estimate. We intentionally fuse each individual "insufficient" measurement immediately as it is obtained. With this approach, we are able to generate estimates more frequently, with less latency, and with improved accuracy, and we are able to estimate the LED positions online concurrently while tracking the HiBall (section 5.4).</p> <p>Welch 2001 at Section 5.3.</p> <p>We use a Kalman filter (Kalman, 1960) to fuse the measurements into an estimate of the HiBall state x (the pose of the HiBall). We use the Kalman filter—a minimum-variance stochastic estimator—both because the sensor measurement noise and the typical user-motion dynamics can be modeled as normally distributed</p>

Exhibit E-6

CLAIM 1	Welch 2001
	<p>random processes, and because we want an efficient online method of estimation.</p> <p>Welch 2001 at Section 5.3.</p> <p>The Kalman filter has been used previously to address similar or related problems. . . . A relevant example of a Kalman filter used for sensor fusion in a wide-area tracking system is given in Foxlin et al. (1998), which describes a hybrid inertial-acoustic system that is commercially available today (Intersense, 2000). Welch 2001 at Section 5.3.</p> <p>[O]ne key benefit warrants discussion here. There is a direct relationship between the complexity of the estimation algorithm, the corresponding speed (execution time per estimation cycle), and the change in HiBall pose between estimation cycles (figure 12). As the algorithmic complexity increases, the execution time increases, which allows for significant nonlinear HiBall motion between estimation cycles, which in turn implies the need for a more complex estimation algorithm. Welch 2001 at Section 5.3.</p>

Exhibit E-6


CLAIM 1	Welch 2001
	<div data-bbox="506 240 1129 933">  <p data-bbox="506 893 651 933">Figure 12.</p> </div> <p data-bbox="499 971 1961 1187">The SCAAT approach, on the other hand, is an attempt to reverse this cycle. Because we intentionally use a single constraint per estimate, the algorithmic complexity is drastically reduced, which reduces the execution time, and hence the amount of motion between estimation cycles. Because the amount of motion is limited, we are able to use a simple dynamic (process) model in the Kalman filter, which further simplifies the computations. In short, the simplicity of the approach means that it can run very fast, which means it can produce estimates very rapidly, with low noise.</p> <p data-bbox="499 1192 846 1222">Welch 2001 at Section 5.3.</p> <p data-bbox="499 1260 1961 1403">The Kalman filter requires both a model of the process dynamics and a model of the relationship between the process state and the available measurements. In part due to the simplicity of the SCAAT approach, we are able to use a simple position-velocity (PV) process model (Brown & Hwang, 1992). . . . We model the continuous change in the HiBall state with the simple differential equation</p>

Exhibit E-6

CLAIM 1	Welch 2001
	<div data-bbox="506 240 1268 764">$\frac{d}{dt}\tilde{x}(t) = \begin{bmatrix} 0 & 1 \\ 0 & 0 \end{bmatrix} \begin{bmatrix} x_p(t) \\ x_v(t) \end{bmatrix} + \begin{bmatrix} 0 \\ \mu \end{bmatrix} u(t), \quad (1)$<p>where $u(t)$ is a normally distributed white (in the frequency spectrum) scalar noise process, and the scalar μ represents the magnitude or spectral density of the noise. We use a similar model with a distinct noise process for each of the six pose elements. We determine the individual noise magnitudes using an offline simulation of the system and a nonlinear optimization strategy that seeks to minimize the variance between the estimated pose and a known motion path. (See section 6.2.2.).</p></div> <p data-bbox="506 805 846 837">Welch 2001 at Section 5.3.</p> <p data-bbox="506 873 1967 1019">The differential equation (1) represents a continuous integrated random walk, or an integrated Wiener or Brownian-motion process. Specifically, we model each component of the linear and angular HiBall velocities as a random walk, and then use these (assuming constant intermeasurement velocity) to estimate the HiBall pose at time $t + \delta t$ as follows:</p>

Exhibit E-6

CLAIM 1	Welch 2001
	<div data-bbox="730 266 1255 337" data-label="Equation-Block"> $\bar{x}(t + \delta t) = \begin{bmatrix} 1 & \delta t \\ 0 & 1 \end{bmatrix} \bar{x}(t) \quad (2)$ </div> <p data-bbox="520 380 1247 581">for each of the six pose elements. In addition to a relatively simple process model, the HiBall measurement model is relatively simple. For any ceiling LED (section 4.2) and HiBall view (section 4.1), the 2-D sensor measurement can be modeled as</p> <div data-bbox="793 623 1255 695" data-label="Equation-Block"> $\begin{bmatrix} u \\ v \end{bmatrix} = \begin{bmatrix} c_x/c_z \\ c_y/c_z \end{bmatrix} \quad (3)$ </div> <p data-bbox="520 737 600 769">where</p> <div data-bbox="739 812 1255 915" data-label="Equation-Block"> $\begin{bmatrix} c_x \\ c_y \\ c_z \end{bmatrix} = VR^T(\bar{l}_{xyz} - \bar{x}_{xyz}), \quad (4)$ </div> <p data-bbox="520 958 1247 1295">V is the camera viewing matrix from section 5.1, \bar{l}_{xyz} is the position of the LED in the world, \bar{x}_{xyz} is the position of the HiBall in the world, and R is a rotation matrix corresponding to the orientation of the HiBall in the world. In practice, we maintain the orientation of the HiBall as a combination of a global (external to the state) quaternion and a set of incremental angles as described by Welch (1996) and Welch and Bishop (1997).</p> <p data-bbox="504 1344 844 1377">Welch 2001 at Section 5.3.</p>

Exhibit E-6

CLAIM 1	Welch 2001
	<p>Because the measurement model (3) and (4) is non-linear, we use an extended Kalman filter, making use of the Jacobian of the nonlinear HiBall measurement model to transform the covariance of the Kalman filter. Welch 2001 at Section 5.3.</p> <p>Along with the benefit of simplicity and speed, the SCAAT approach offers the additional capability of being able to estimate the 3-D positions of the LEDs in the world concurrently with the pose of the HiBall, online, in real time. This capability is a tremendous benefit in terms of the accuracy and noise characteristics of the estimates.</p>

Exhibit E-6

CLAIM 1	Welch 2001
	<p data-bbox="520 248 1262 1109">The method we now use for autocalibration involves defining a distinct SCAAT Kalman filter for each LED. Specifically, for each LED, we maintain a state \bar{l} (estimate of the 3-D position) and a 3×3 Kalman filter covariance. At the beginning of each estimation cycle, we form an augmented state vector \hat{x} using the appropriate LED state and the current HiBall state: $\hat{x} = [\bar{x}^T, \bar{l}^T]^T$. Similarly, we augment the Kalman filter error covariance matrix with that of the LED filter. We then follow the normal steps outlined in section 5.3, with the result being that the LED portion of the filter state and covariance is updated in accordance with the measurement residual. At the end of the cycle, we extract the LED portions of the state and covariance from the augmented filter, and save them externally. The effect is that, as the system is being used, it continually refines its estimates of the LED positions, thereby continually improving its estimates of the HiBall pose. Again, for additional information, see Welch (1996) and Welch and Bishop (1997).</p> <p data-bbox="520 1157 846 1190">Welch 2001 at Section 5.4.</p> <p data-bbox="520 1227 1944 1369">The recursive nature of the Kalman filter (section 5.3) requires that the filter be initialized with a known state and corresponding covariance before steady-state operation can begin. Such an initialization (or acquisition) must take place prior to any tracking session, but also upon the (rare) occasion when the filter diverges and “loses lock” as a result of blocked sensor views, for example.</p> <p data-bbox="520 1373 846 1406">Welch 2001 at Section 5.5.</p>

Exhibit E-6

CLAIM 1	Welch 2001
	<i>See also</i> Defendants' Invalidity Contentions for further discussion.
[1.b] a sensor subsystem coupled to the estimation subsystem and configured to provide configuration data to the estimation subsystem and to provide measurement information to the estimation subsystem for localizing an object;	<p>At least under Plaintiffs' apparent infringement theory, Welch 2001 discloses, either expressly or inherently, a sensor subsystem coupled to the estimation subsystem and configured to provide configuration data to the estimation subsystem and to provide measurement information to the estimation subsystem for localizing an object. In the alternative, this element would be obvious over Welch 2001 in light of the other references disclosed in Defendants' Invalidity Contentions and/or the knowledge of one of ordinary skill in the art.</p> <p><i>See, e.g.:</i></p> <p>In all of the optical systems we have developed (see section 1.2), we have chosen what we call an inside-looking-out configuration, in which the optical sensors are on the (moving) user and the landmarks (for instance, the LEDs) are fixed in the laboratory. The corresponding outside-looking-in alternative would be to place the landmarks on the user and to fix the optical sensors in the laboratory. (One can think about similar outside-in and inside-out distinctions for acoustic and magnetic technologies.) The two configurations are depicted in figure 5. Welch 2001 at Section 2.</p>

Exhibit E-6

CLAIM 1	Welch 2001
	<div data-bbox="506 240 1654 906"> <p>Figure 5 illustrates two head tracking configurations. The 'Outside-Looking-In' configuration on the left shows a user wearing a head-mounted device with landmarks. A 'lab-mounted (fixed) optical sensor' is positioned to the left, with dashed lines indicating its field of view over the landmarks. The 'Inside-Looking-Out' configuration on the right shows a user wearing a 'head-mounted sensor'. Above the user, a horizontal bar holds several 'lab-mounted (fixed) landmarks'. Dashed lines show the sensor's field of view directed at these landmarks.</p> </div> <p>[T]here are fewer mechanical considerations when mounting sensors in the environment for an outside-looking-in configuration. Because landmarks can be relatively simple, small, and cheap, they can often be located in numerous places on the user, and communication from the user to the rest of the system can be relatively simple or even unnecessary. This is particularly attractive for full-body motion capture. Welch 2001 at Section 2.</p> <p>However, there are some significant advantages to the inside-looking-out approach for head tracking. By operating with sensors on the user rather than in the environment, the system can be scaled indefinitely. . . . The inside-looking-out configuration is also motivated by a desire to maximize sensitivity to changes in user pose. Welch 2001 at Section 2.</p> <p>The HiBall Tracking System consists of three main components (figure 6). An outward-looking sensing unit we call the HiBall is fixed to each user to be tracked. The HiBall unit observes a subsystem of fixed-location infrared LEDs we call the Ceiling. Communication and synchronization between the host computer and</p>

Exhibit E-6

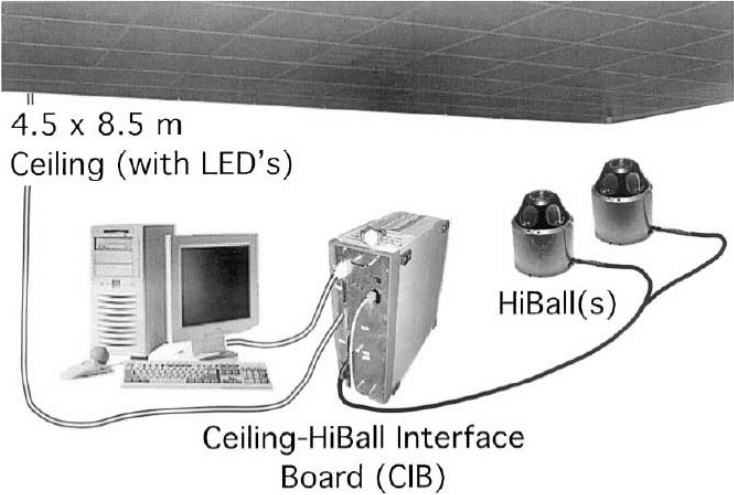
CLAIM 1	Welch 2001
	<p>these subsystems is coordinated by the Ceiling-HiBall Interface Board (CIB). Welch 2001 at Section 3.</p> <p>HiBall observes LEDs through multiple sensor-lens views that are distributed over a large solid angle. LEDs are sequentially flashed (one at a time) such that they are seen via a diverse set of views for each HiBall. Initial acquisition is performed using a brute-force search through LED space, but, once initial lock is made, the selection of LEDs to flash is tailored to the views of the active HiBall units. Pose estimates are maintained using a Kalman-filter-based prediction-correction approach known as single-constraint-at-a-time (SCAAT) tracking. This technique has been extended to provide self-calibration of the ceiling, concurrent with HiBall tracking. Welch 2001 at Section 3.</p>  <p>Figure 6.</p> <p>The original electro-optical tracker (figure 3, bottom) used independently housed lateral-effect photodiode units (LEPDs) attached to a lightweight tubular framework. As it turns out, the mechanical framework would flex (distort) during use, contributing to estimation errors. In part to address this problem, the HiBall sensor unit was designed as a single, rigid, hollow ball having dodecahedral symmetry, with lenses in the upper six faces and LEPDs on the insides of the opposing six lower faces (figure 7). This immediately gives six primary “camera”</p>

Exhibit E-6

CLAIM 1	Welch 2001
	<p>views uniformly spaced by 57 deg. The views efficiently share the same internal air space and are rigid with respect to each other. In addition, light entering any lens sufficiently off-axis can be seen by a neighboring LEPD, giving rise to five secondary views through the top or central lens, and three secondary views through the five other lenses. Overall, this provides 26 fields of view that are used to sense widely separated groups of LEDs in the environment. Although the extra views complicate the initialization of the Kalman filter as described in section 5.5, they turn out to be of great benefit during steady-state tracking by effectively increasing the overall HiBall field of view without sacrificing optical-sensor resolution.</p> <p>Welch 2001 at Section 4.1</p> <p>HiBall sensor unit was designed as a single, rigid, hollow ball having dodecahedral symmetry, with lenses in the upper six faces and LEPDs on the insides of the opposing six lower faces (figure 7). This immediately gives six primary “camera” views uniformly spaced by 57 deg. The views efficiently share the same internal air space and are rigid with respect to each other. In addition, light entering any lens sufficiently off-axis can be seen by a neighboring LEPD, giving rise to five secondary views through the top or central lens, and three secondary views through the five other lenses. Overall, this provides 26 fields of view that are used to sense widely separated groups of LEDs in the environment.</p> <p>Welch 2001 at Section 4.1.</p>

Exhibit E-6

CLAIM 1	Welch 2001
	<div data-bbox="512 245 961 683" data-label="Image"> </div> <div data-bbox="512 716 961 1052" data-label="Image"> </div> <div data-bbox="512 1068 634 1101" data-label="Caption"> <p>Figure 7.</p> </div> <div data-bbox="499 1149 1955 1403" data-label="Text"> <p>The LEPDs themselves are not imaging devices; rather, they detect the centroid of the luminous flux incident on the detector. The x-position of the centroid determines the ratio of two output y-position determines the ratio of two other output currents. The total output current of each pair are commensurate and are proportional to the total incident flux. Consequently, focus is not an issue, so the simple fixed-focus lenses work well over a range of LED distances from about half a meter to infinity. The LEPDs and associated electronic components are mounted on a custom rigid-flex printed circuit board (figure 8). This arrangement makes efficient use of the internal HiBall volume while maintaining isolation between analog and digital circuitry, and increasing reliability</p> </div>

Exhibit E-6

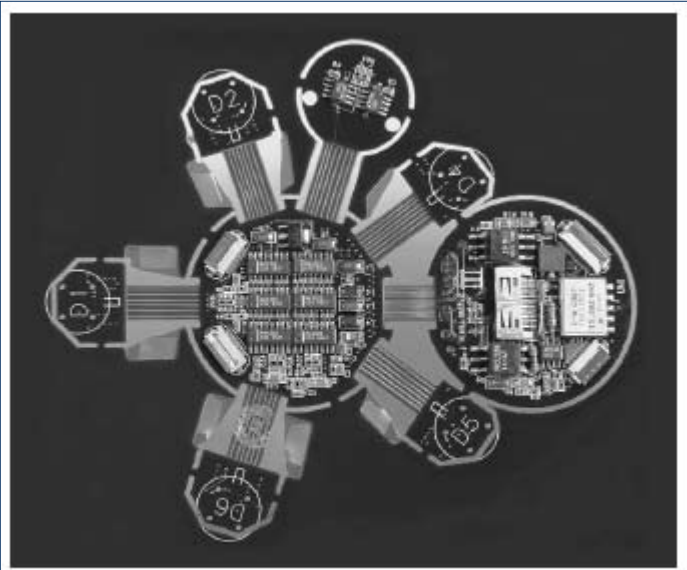
CLAIM 1	Welch 2001
	<p>by alleviating the need for intercomponent mechanical connectors. Welch 2001 at Section 4.1.</p> <div data-bbox="506 345 1188 911">  </div> <p>Figure 8.</p> <p>Figure 9 shows the physical arrangement of the folded electronics in the HiBall. Each LEPD has four transimpedance amplifiers (shown together as one “Amp” in figure 9), the analog outputs of which are multiplexed with those of the other LEPDs, then sampled, held, and converted by four 16-bit Delta-Sigma analog-to-digital (A/D) converters. Multiple samples are integrated via an accumulator. The digitized LEPD data are organized into packets for communication back to the CIB. The packets also contain information to assist in error detection. The communication protocol is simple, and, while presently implemented by wire, the modulation scheme is amenable to a wireless implementation. Welch 2001 at Section 4.1.</p>

Exhibit E-6

CLAIM 1	Welch 2001
	<div data-bbox="506 240 1507 1003"> <p>Figure 9.</p> </div> <p>The design results in a ceiling with a rectangular LED pattern with periods of 7.6 cm and 15.2 cm. This spacing is used for the initial estimates of the LED positions in the lab; then, during normal operation, the SCAAT algorithm continually refines the LED position estimates (section 5.4). The SCAAT autocalibration not only relaxes design and installation constraints, but provides greater precision in the face of initial and ongoing uncertainty in the ceiling structure.</p> <p>Welch 2001 at Section 4.2.</p> <p>The Ceiling-HiBall Interface Board (CIB) (figure 11) provides communication and synchronization between a host personal computer, the HiBall (section 4.1), and the ceiling (section 4.2). The CIB has four ceiling ports allowing interleaving of ceiling panels for up to four simultaneous LED flashes and/or higher ceiling bandwidth. (The ceiling bandwidth is inherently limited by LED power restrictions as described in section 4.2, but this can be</p>

Exhibit E-6

CLAIM 1	Welch 2001
	<p>increased by spatially multiplexing the ceiling panels.) The CIB has two tether interfaces that can communicate with up to four daisy-chained HiBall units. The full-duplex communication with the HiBall units uses a modulation scheme (BPSK) allowing future wireless operation. The interface from the CIB to the host PC is the stable IEEE1284C extended parallel port (EPP) standard.</p> <p>The CIB comprises analog drive and receive components as well as digital logic components. The digital components implement store and forward in both directions and synchronize the timing of the LED “on” interval within the HiBall dark-light-dark intervals (section 5.2). The protocol supports full-duplex flow control. The data are arranged into packets that incorporate error detection.</p> <p>Welch 2001 at Section 4.3.</p> <p>After each HiBall is assembled, we perform an offline calibration procedure to determine the correspondence between image-plane coordinates and rays in space. This involves more than just determining the view transform for each of the 26 views. Nonlinearities in the silicon sensor and distortions in the lens (such as spherical aberration) cause significant deviations from a simple pinhole camera model. We dealt with all of these issues through the use of a two-part camera model. The first part is a standard pinhole camera represented by a 3 X 4 matrix. The second part is a table mapping real image-plane coordinates to ideal image-plane coordinates.</p> <p>Welch 2001 at Section 5.1.</p> <p>Both parts of the camera model are determined using a calibration procedure that relies on a goniometer (an angular positioning system) of our own design. This device consists of two servo motors mounted together such that one motor provides rotation about the vertical axis while the second motor provides rotation about an axis orthogonal to vertical. An important characteristic of the goniometer is that the rotational axes of the two motors intersect at a point at the center of the HiBall optical sphere; this point is defined as the origin of the HiBall. . . . The rotational positioning motors were rated to provide twenty arc-second precision; we further calibrated them to six arc seconds using a laboratory grade theodolite—an angle measuring system.</p> <p>Welch 2001 at Section 5.1.</p> <p>To determine the mapping between sensor image-plane coordinates and three-space rays, we use a single LED mounted at a fixed location in the laboratory such that it is centered in the view directly out of the top lens of the HiBall. This ray defines the z or up axis for the HiBall coordinate system. We sample other rays by rotating the goniometer motors under computer control. We sample each view with rays spaced about every six minutes of arc throughout the field of view. We repeat each measurement 100 times to reduce the effects of noise on the</p>

Exhibit E-6

CLAIM 1	Welch 2001
	<p>individual measurements and to estimate the standard deviation of the measurements. Welch 2001 at Section 5.1.</p> <p>Given the tables of approximately 2,500 measurements for each of the 26 views, we first determine a 3 X 4 view matrix using standard linear least-squares techniques. Then, we determine the deviation of each measured point from that predicted by the ideal linear model. These deviations are resampled into a 25 X 25 grid indexed by sensor-plane coordinates using a simple scan-conversion procedure and averaging. Given a measurement from a sensor at runtime (section 5.2), we convert it to an “ideal” measurement by subtracting a deviation bilinearly interpolated from the nearest four entries in the table.</p> <p>Welch 2001 at Section 5.1.</p> <p>Upon receiving a command from the CIB (section 4.3), which is synchronized with a CIB command to the ceiling, the HiBall selects the specified LEPD and performs three measurements, one before the LED flashes, one during the LED flash, and one after the LED flash. Known as “dark-light-dark,” this technique is used to subtract out DC bias, low-frequency noise, and background light from the LED signal. We then convert the measured sensor coordinates to “ideal” coordinates using the calibration tables described in section 5.1.</p> <p>In addition, during runtime we attempt to maximize the signal-to-noise ratio of the measurement with an automatic gain-control scheme. For each LED, we store a target signal strength factor. We compute the LED current and number of integrations (of successive accumulated A/D samples) by dividing this strength factor by the square of the distance to the LED, estimated from the current position estimate. After a reading, we look at the strength of the actual measurement. If it is larger than expected, we reduce the gain; if it is less than expected, we increase the gain. The increase and decrease are implemented as online averages with scaling such that the gain factor decreases rapidly (to avoid overflow) and increases slowly. Finally, we use the measured signal strength to estimate the noise on the signal using (Chi, 1995), and then use this as the measurement noise estimate for the Kalman filter (section 5.3).</p> <p>Welch 2001 at Section 5.2.</p> <p>The online measurements (section 5.2) are used to estimate the pose of the HiBall during operation. The 1991 system collected a group of diverse measurements for a variety of LEDs and sensors, and then used a method of simultaneous nonlinear equations called collinearity (Azuma & Ward, 1991) to estimate the pose of the sensor fixture shown in figure 3 (bottom).</p> <p>Welch 2001 at Section 5.3.</p>

Exhibit E-6

CLAIM 1	Welch 2001
	<p>In contrast, the approach we use with the new HiBall system produces tracker reports as each new measurement is made, rather than waiting to form a complete collection of observations. Because single measurements under constrain the mathematical solution, we refer to the approach as single-constraint-at-a-time (SCAAT) tracking (Welch, 1996; Welch & Bishop, 1997). The key is that the single measurements provide some information about the HiBall's state, and thus can be used to incrementally improve a previous estimate. We intentionally fuse each individual "insufficient" measurement immediately as it is obtained. With this approach, we are able to generate estimates more frequently, with less latency, and with improved accuracy, and we are able to estimate the LED positions online concurrently while tracking the HiBall (section 5.4).</p> <p>Welch 2001 at Section 5.3.</p> <p>We use a Kalman filter (Kalman, 1960) to fuse the measurements into an estimate of the HiBall state x (the pose of the HiBall). We use the Kalman filter—a minimum-variance stochastic estimator—both because the sensor measurement noise and the typical user-motion dynamics can be modeled as normally distributed random processes, and because we want an efficient online method of estimation.</p> <p>Welch 2001 at Section 5.3.</p> <p>The Kalman filter has been used previously to address similar or related problems. . . . A relevant example of a Kalman filter used for sensor fusion in a wide-area tracking system is given in Foxlin et al. (1998), which describes a hybrid inertial-acoustic system that is commercially available today (Intersense, 2000).</p> <p>Welch 2001 at Section 5.3.</p> <p>[O]ne key benefit warrants discussion here. There is a direct relationship between the complexity of the estimation algorithm, the corresponding speed (execution time per estimation cycle), and the change in HiBall pose between estimation cycles (figure 12). As the algorithmic complexity increases, the execution time increases, which allows for significant nonlinear HiBall motion between estimation cycles, which in turn implies the need for a more complex estimation algorithm.</p> <p>Welch 2001 at Section 5.3.</p>

Exhibit E-6


CLAIM 1	Welch 2001
	<div data-bbox="506 240 1129 933">  <p data-bbox="506 893 651 933">Figure 12.</p> </div> <p data-bbox="499 971 1961 1187">The SCAAT approach, on the other hand, is an attempt to reverse this cycle. Because we intentionally use a single constraint per estimate, the algorithmic complexity is drastically reduced, which reduces the execution time, and hence the amount of motion between estimation cycles. Because the amount of motion is limited, we are able to use a simple dynamic (process) model in the Kalman filter, which further simplifies the computations. In short, the simplicity of the approach means that it can run very fast, which means it can produce estimates very rapidly, with low noise.</p> <p data-bbox="499 1192 846 1222">Welch 2001 at Section 5.3.</p> <p data-bbox="499 1260 1961 1403">The Kalman filter requires both a model of the process dynamics and a model of the relationship between the process state and the available measurements. In part due to the simplicity of the SCAAT approach, we are able to use a simple position-velocity (PV) process model (Brown & Hwang, 1992). . . . We model the continuous change in the HiBall state with the simple differential equation</p>

Exhibit E-6

CLAIM 1	Welch 2001
	<div data-bbox="506 240 1268 764">$\frac{d}{dt}\bar{x}(t) = \begin{bmatrix} 0 & 1 \\ 0 & 0 \end{bmatrix} \begin{bmatrix} x_p(t) \\ x_v(t) \end{bmatrix} + \begin{bmatrix} 0 \\ \mu \end{bmatrix} u(t), \quad (1)$<p>where $u(t)$ is a normally distributed white (in the frequency spectrum) scalar noise process, and the scalar μ represents the magnitude or spectral density of the noise. We use a similar model with a distinct noise process for each of the six pose elements. We determine the individual noise magnitudes using an offline simulation of the system and a nonlinear optimization strategy that seeks to minimize the variance between the estimated pose and a known motion path. (See section 6.2.2.).</p></div> <p data-bbox="506 805 846 836">Welch 2001 at Section 5.3.</p> <p data-bbox="506 873 1967 1019">The differential equation (1) represents a continuous integrated random walk, or an integrated Wiener or Brownian-motion process. Specifically, we model each component of the linear and angular HiBall velocities as a random walk, and then use these (assuming constant intermeasurement velocity) to estimate the HiBall pose at time $t + \delta t$ as follows:</p>

Exhibit E-6

CLAIM 1	Welch 2001
	<div data-bbox="730 266 1255 337" data-label="Equation-Block"> $\bar{x}(t + \delta t) = \begin{bmatrix} 1 & \delta t \\ 0 & 1 \end{bmatrix} \bar{x}(t) \quad (2)$ </div> <p data-bbox="520 378 1249 581">for each of the six pose elements. In addition to a relatively simple process model, the HiBall measurement model is relatively simple. For any ceiling LED (section 4.2) and HiBall view (section 4.1), the 2-D sensor measurement can be modeled as</p> <div data-bbox="793 623 1255 695" data-label="Equation-Block"> $\begin{bmatrix} u \\ v \end{bmatrix} = \begin{bmatrix} c_x/c_z \\ c_y/c_z \end{bmatrix} \quad (3)$ </div> <p data-bbox="520 735 600 768">where</p> <div data-bbox="737 812 1255 915" data-label="Equation-Block"> $\begin{bmatrix} c_x \\ c_y \\ c_z \end{bmatrix} = VR^T(\bar{l}_{xyz} - \bar{x}_{xyz}), \quad (4)$ </div> <p data-bbox="520 958 1249 1295">V is the camera viewing matrix from section 5.1, \bar{l}_{xyz} is the position of the LED in the world, \bar{x}_{xyz} is the position of the HiBall in the world, and R is a rotation matrix corresponding to the orientation of the HiBall in the world. In practice, we maintain the orientation of the HiBall as a combination of a global (external to the state) quaternion and a set of incremental angles as described by Welch (1996) and Welch and Bishop (1997).</p> <p data-bbox="504 1344 844 1377">Welch 2001 at Section 5.3.</p>

Exhibit E-6

CLAIM 1	Welch 2001
	<p>Because the measurement model (3) and (4) is non-linear, we use an extended Kalman filter, making use of the Jacobian of the nonlinear HiBall measurement model to transform the covariance of the Kalman filter. Welch 2001 at Section 5.3.</p> <p>Along with the benefit of simplicity and speed, the SCAAT approach offers the additional capability of being able to estimate the 3-D positions of the LEDs in the world concurrently with the pose of the HiBall, online, in real time. This capability is a tremendous benefit in terms of the accuracy and noise characteristics of the estimates.</p>

Exhibit E-6

CLAIM 1	Welch 2001
	<p data-bbox="506 248 1268 1109"> The method we now use for autocalibration involves defining a distinct SCAAT Kalman filter for each LED. Specifically, for each LED, we maintain a state \bar{l} (estimate of the 3-D position) and a 3×3 Kalman filter covariance. At the beginning of each estimation cycle, we form an augmented state vector \hat{x} using the appropriate LED state and the current HiBall state: $\hat{x} = [\bar{x}^T, \bar{l}^T]^T$. Similarly, we augment the Kalman filter error covariance matrix with that of the LED filter. We then follow the normal steps outlined in section 5.3, with the result being that the LED portion of the filter state and covariance is updated in accordance with the measurement residual. At the end of the cycle, we extract the LED portions of the state and covariance from the augmented filter, and save them externally. The effect is that, as the system is being used, it continually refines its estimates of the LED positions, thereby continually improving its estimates of the HiBall pose. Again, for additional information, see Welch (1996) and Welch and Bishop (1997). </p> <p data-bbox="506 1159 848 1187">Welch 2001 at Section 5.4.</p> <p data-bbox="506 1227 1944 1369"> The recursive nature of the Kalman filter (section 5.3) requires that the filter be initialized with a known state and corresponding covariance before steady-state operation can begin. Such an initialization (or acquisition) must take place prior to any tracking session, but also upon the (rare) occasion when the filter diverges and “loses lock” as a result of blocked sensor views, for example. </p> <p data-bbox="506 1377 848 1404">Welch 2001 at Section 5.5.</p>

Exhibit E-6


CLAIM 1	Welch 2001
	<p data-bbox="499 240 1955 418">The acquisition process is complicated by the fact that each LEPD sees a number of different widely separated views (section 4.1). Therefore, detecting an LED provides at best an ambiguous set of potential LED directions in HiBall coordinates. Moreover, before acquisition, no assumptions can be made to limit the search space of visible LEDs. As such, a relatively slow brute-force algorithm is used to acquire lock. Welch 2001 at Section 5.5.</p> <p data-bbox="499 456 1955 818">As a result of a mechanical design tradeoff, each sensor field of view is less than six degrees. The focal length is set by the size of the sensor housing, which is set by the diameter of the sensors themselves. Energetics is also a factor, limiting how small the lenses can be while maintaining sufficient light-collecting area. As a result of these design tradeoffs, even a momentary small error in the HiBall pose estimate can cause the recursive estimates to diverge and the system to lose lock after only a few LED sightings. And yet the system is quite robust. In practice, users can jump around, crawl on the floor, lean over, even wave their hands in front of the sensors, and the system does not lose lock. During one session, we were using the HiBall as a 3-D digitization probe, a Hi-Ball on the end of a pencil-shaped fiberglass wand (figure 14, left). We laid the probe down on a table at one point, and were amazed to later notice that it was still tracking, even though it was observing only three or four LEDs near the edge of the ceiling. We picked up the probe and continued using it, without it ever losing lock.</p> <div data-bbox="506 852 1129 1149"><p data-bbox="514 1109 646 1138">Figure 13.</p></div>

Exhibit E-6

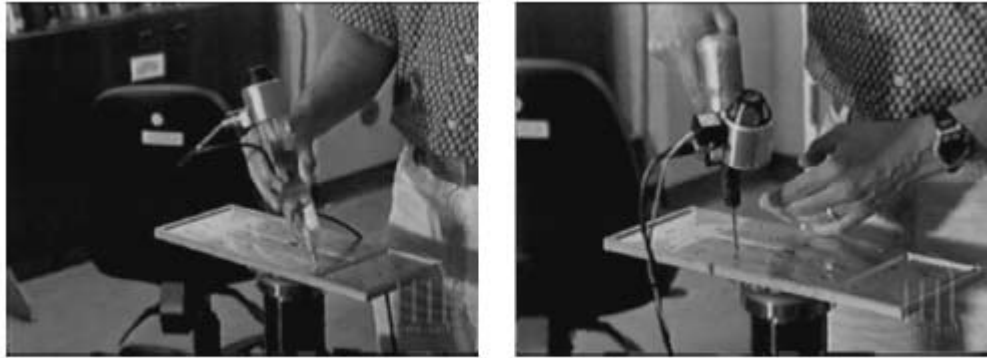
CLAIM 1	Welch 2001
	<div data-bbox="512 250 1493 605">  </div> <p data-bbox="512 626 646 656">Figure 14.</p> <p data-bbox="499 719 846 748">Welch 2001 at Section 6.1.</p> <p data-bbox="499 789 1961 1036">To make measurements of the noise when the HiBall is in motion, we rely on the assumption that almost all of the signal resulting from normal human motion is at frequencies below 2 Hz. We use a high-pass filter (Welch, 1967) on the pose estimates, and assume the output is noise. The resulting statistics are comparable to those made with the HiBall stationary, except at poses for which there are very few LEDs visible in only one or two views. In these poses, near the edge of the ceiling, the geometry of the constraints results in amplification of errors. For nearly all of the working volume of the tracker, the standard deviation of the noise on measurements while the HiBall is still or moving is about 0.2 mm and 0.03 deg.</p> <p data-bbox="499 1044 846 1073">Welch 2001 at Section 6.1.</p> <p data-bbox="499 1114 1961 1219">During the design of the HiBall system, we made substantial use of simulation, in some domains to a very detailed level. For example, Zemax (Focus Software, 1995) was used extensively in the design and optimization of the optical design, including the design of the filter glass lenses, and geometry of the optical-component layout.</p> <p data-bbox="499 1227 846 1256">Welch 2001 at Section 6.2.</p> <p data-bbox="499 1297 1961 1464">To produce realistic data for developing and tuning our algorithms, we collected several motion paths (sequences of pose estimates) from our first-generation electro-optical tracker (figure 3) at its 70 Hz maximum report rate. These paths were recorded from both naive users visiting our monthly “demo days” and from experienced users in our labs. . . . we filtered the raw path data with a noncausal zero-phase-shift, low-pass filter to eliminate energy above 2 Hz. The output of the low-pass filtering was then resampled at whatever rate we wanted to run the</p>

Exhibit E-6

CLAIM 1	Welch 2001
	<p>simulated tracker, usually 1,000 Hz. Welch 2001 at Section 6.2.</p> <p>The simulator reads camera models describing the 26 views, the sensor noise parameters, the LED positions and their expected error, and the motion path described above. Before beginning the simulation, the LED positions are perturbed from their ideal positions by adding normally distributed error to each axis. Then, for each simulated cycle of operation, the “true” poses are up- dated using the input motion path. Next, a view is chosen and a visible LED within that view is selected, and the image-plane coordinates of the LED on the chosen sensor are computed using the camera model for the view and the LED as described in section 5.3. These sensor coordinates are then perturbed based on the sensor noise model (section 6.2.1) using the distance and angle to the LED. These noise-corrupted sensor readings are then fed to the SCAAT filter to produce an updated position estimate. The position estimate is compared to the true position to produce a scalar error metric that is described next. Welch 2001 at Section 6.2.</p> <p>The error metric we used combines the error in pose in a way that relates to the effects of tracker error on a head-worn display user. We define a set of points arrayed around the user in a fixed configuration. We compute two sets of coordinates for these points: the true position using the true pose and their estimated position using the estimated pose. The error metric is then the sum of the distances between the true and estimated positions of these points. By adjusting the distance of the points from the user, we can control the relative importance of the orientation and the position error in the combined error metric. If the distance is small, then the position error is weighted most heavily; if the distance is large, then the orientation error is weighted most heavily. Our two error metrics for the entire run are the square root of the sum of the squares of all the distances, and the peak distance. Welch 2001 at Section 6.2.</p> <p><i>See also</i> Defendants’ Invalidity Contentions for further discussion.</p>
[1.c] wherein the estimation subsystem is configured to update a location estimate for the object based on configuration data and	<p>At least under Plaintiffs’ apparent infringement theory, Welch 2001 discloses, either expressly or inherently, wherein the estimation subsystem is configured to update a location estimate for the object based on configuration data and measurement information accepted from the sensor subsystem. In the alternative, this element would be obvious over Welch 2001 in light of the other references disclosed in Defendants’ Invalidity Contentions and/or the knowledge of one of ordinary skill in the art.</p>

Exhibit E-6

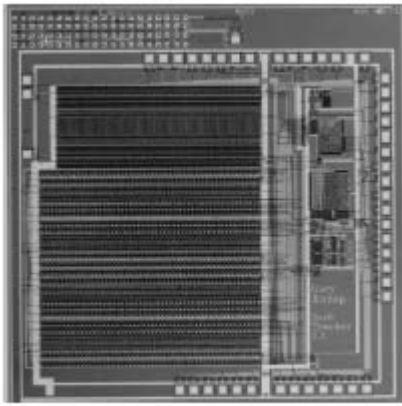
CLAIM 1	Welch 2001
<p>measurement information accepted from the sensor subsystem.</p>	<p><i>See, e.g.:</i></p> <p>As part of his 1984 dissertation on Self-Tracker, Bishop put forward the idea of outward-looking tracking systems based on user-mounted sensors that estimate user pose by observing landmarks in the environment (Bishop, 1984). He described two kinds of landmarks: high signal-to-noise-ratio beacons such as light-emitting diodes (LEDs) and low signal-to-noise- ratio landmarks such as naturally occurring features. Bishop designed and demonstrated custom VLSI chips (figure 2) that combined image sensing and processing on a single chip (Bishop & Fuchs, 1984). The idea was to combine multiple instances of these chips into an outward-looking cluster that estimated cluster motion by observing natural features in the unmodified environment. Integrating the resulting motion to estimate pose is prone to accumulating error, so further development required a complementary system based on easily detectable landmarks (LEDs) at known locations.</p> <p>Welch 2001 at Section 1.2.</p> <div data-bbox="506 706 947 1190"><p>Figure 2.</p></div> <p>As a result of these improvements, the HiBall Tracking System can generate more than 2,000 pose estimates per second, with less than 1 ms of latency, better than 0.5 mm and 0.03 deg. of absolute error and noise, everywhere in a 4.5 m x 8.5 m room (with more than two meters of height variation). The area can be expanded by adding more panels, or by using checker-board configurations that spread panels over a larger area. The weight of the user-worn HiBall is approximately 300 grams, making it lighter than one optical sensor in the 1991 system. Multiple</p>

Exhibit E-6

CLAIM 1	Welch 2001
	<p>HiBall units can be daisy-chained together for head or hand tracking, pose-aware input devices, or precise 3-D point digitization throughout the entire working volume.</p> <p>Welch 2001 at Section 1.3.</p> <p>In this article, we describe a new and vastly improved version of the 1991 system. We call the new system the HiBall Tracking System. Thanks to significant improvements in hardware and software, this HiBall system offers unprecedented speed, resolution, accuracy, robustness, and flexibility. The bulky and heavy sensors and backpack of the previous system have been replaced by a small HiBall unit (figure 4, bottom). In addition, the precisely machined LED ceiling panels of the previous system have been replaced by looser-tolerance panels that are relatively inexpensive to make and simple to install (figure 4, top; figure 10). Finally, we are using an unusual Kalman-filter-based algorithm that generates very accurate pose estimates at a high rate with low latency, and that simultaneously self-calibrates the system.</p> <p>Welch 2001 at Section 1.3.</p> <p>HiBall observes LEDs through multiple sensor-lens views that are distributed over a large solid angle. LEDs are sequentially flashed (one at a time) such that they are seen via a diverse set of views for each HiBall. Initial acquisition is performed using a brute-force search through LED space, but, once initial lock is made, the selection of LEDs to flash is tailored to the views of the active HiBall units. Pose estimates are maintained using a Kalman-filter-based prediction-correction approach known as single-constraint-at-a-time (SCAAT) tracking. This technique has been extended to provide self-calibration of the ceiling, concurrent with HiBall tracking.</p> <p>Welch 2001 at Section 3.</p> <p>The design results in a ceiling with a rectangular LED pattern with periods of 7.6 cm and 15.2 cm. This spacing is used for the initial estimates of the LED positions in the lab; then, during normal operation, the SCAAT algorithm continually refines the LED position estimates (section 5.4). The SCAAT autocalibration not only relaxes design and installation constraints, but provides greater precision in the face of initial and ongoing uncertainty in the ceiling structure.</p> <p>Welch 2001 at Section 4.2.</p> <p>To determine the mapping between sensor image-plane coordinates and three-space rays, we use a single LED mounted at a fixed location in the laboratory such that it is centered in the view directly out of the top lens of the</p>

Exhibit E-6

CLAIM 1	Welch 2001
	<p>HiBall. This ray defines the z or up axis for the HiBall coordinate system. We sample other rays by rotating the goniometer motors under computer control. We sample each view with rays spaced about every six minutes of arc throughout the field of view. We repeat each measurement 100 times to reduce the effects of noise on the individual measurements and to estimate the standard deviation of the measurements. Welch 2001 at Section 5.1.</p> <p>Given the tables of approximately 2,500 measurements for each of the 26 views, we first determine a 3 X 4 view matrix using standard linear least-squares techniques. Then, we determine the deviation of each measured point from that predicted by the ideal linear model. These deviations are resampled into a 25 X 25 grid indexed by sensor-plane coordinates using a simple scan-conversion procedure and averaging. Given a measurement from a sensor at runtime (section 5.2), we convert it to an “ideal” measurement by subtracting a deviation bilinearly interpolated from the nearest four entries in the table. Welch 2001 at Section 5.1.</p> <p>Upon receiving a command from the CIB (section 4.3), which is synchronized with a CIB command to the ceiling, the HiBall selects the specified LEPD and performs three measurements, one before the LED flashes, one during the LED flash, and one after the LED flash. Known as “dark-light-dark,” this technique is used to subtract out DC bias, low-frequency noise, and background light from the LED signal. We then convert the measured sensor coordinates to “ideal” coordinates using the calibration tables described in section 5.1.</p> <p>In addition, during runtime we attempt to maximize the signal-to-noise ratio of the measurement with an automatic gain-control scheme. For each LED, we store a target signal strength factor. We compute the LED current and number of integrations (of successive accumulated A/D samples) by dividing this strength factor by the square of the distance to the LED, estimated from the current position estimate. After a reading, we look at the strength of the actual measurement. If it is larger than expected, we reduce the gain; if it is less than expected, we increase the gain. The increase and decrease are implemented as online averages with scaling such that the gain factor decreases rapidly (to avoid overflow) and increases slowly. Finally, we use the measured signal strength to estimate the noise on the signal using (Chi, 1995), and then use this as the measurement noise estimate for the Kalman filter (section 5.3). Welch 2001 at Section 5.2.</p> <p>The online measurements (section 5.2) are used to estimate the pose of the HiBall during operation. The 1991 system collected a group of diverse measurements for a variety of LEDs and sensors, and then used a method of simultaneous nonlinear equations called collinearity (Azuma & Ward, 1991) to estimate the pose</p>

Exhibit E-6

CLAIM 1	Welch 2001
	<p data-bbox="499 240 1150 272">of the sensor fixture shown in figure 3 (bottom).</p> <p data-bbox="499 277 846 310">Welch 2001 at Section 5.3.</p> <p data-bbox="499 345 1963 670">In contrast, the approach we use with the new HiBall system produces tracker reports as each new measurement is made, rather than waiting to form a complete collection of observations. Because single measurements under constrain the mathematical solution, we refer to the approach as single-constraint-at-a-time (SCAAT) tracking (Welch, 1996; Welch & Bishop, 1997). The key is that the single measurements provide some information about the HiBall’s state, and thus can be used to incrementally improve a previous estimate. We intentionally fuse each individual “insufficient” measurement immediately as it is obtained. With this approach, we are able to generate estimates more frequently, with less latency, and with improved accuracy, and we are able to estimate the LED positions online concurrently while tracking the HiBall (section 5.4).</p> <p data-bbox="499 675 846 708">Welch 2001 at Section 5.3.</p> <p data-bbox="499 743 1963 881">We use a Kalman filter (Kalman, 1960) to fuse the measurements into an estimate of the HiBall state x (the pose of the HiBall). We use the Kalman filter—a minimum-variance stochastic estimator—both because the sensor measurement noise and the typical user-motion dynamics can be modeled as normally distributed random processes, and because we want an efficient online method of estimation.</p> <p data-bbox="499 886 846 919">Welch 2001 at Section 5.3.</p> <p data-bbox="499 954 1917 1060">The Kalman filter has been used previously to address similar or related problems. . . . A relevant example of a Kalman filter used for sensor fusion in a wide-area tracking system is given in Foxlin et al. (1998), which describes a hybrid inertial-acoustic system that is commercially available today (Intersense, 2000).</p> <p data-bbox="499 1065 846 1097">Welch 2001 at Section 5.3.</p> <p data-bbox="499 1133 1963 1312">[O]ne key benefit warrants discussion here. There is a direct relationship between the complexity of the estimation algorithm, the corresponding speed (execution time per estimation cycle), and the change in HiBall pose between estimation cycles (figure 12). As the algorithmic complexity increases, the execution time increases, which allows for significant nonlinear HiBall motion between estimation cycles, which in turn implies the need for a more complex estimation algorithm.</p> <p data-bbox="499 1317 846 1349">Welch 2001 at Section 5.3.</p>

Exhibit E-6


CLAIM 1	Welch 2001
	<div data-bbox="506 240 1129 933">  <p data-bbox="506 893 651 933">Figure 12.</p> </div> <p data-bbox="499 971 1961 1187">The SCAAT approach, on the other hand, is an attempt to reverse this cycle. Because we intentionally use a single constraint per estimate, the algorithmic complexity is drastically reduced, which reduces the execution time, and hence the amount of motion between estimation cycles. Because the amount of motion is limited, we are able to use a simple dynamic (process) model in the Kalman filter, which further simplifies the computations. In short, the simplicity of the approach means that it can run very fast, which means it can produce estimates very rapidly, with low noise.</p> <p data-bbox="499 1192 846 1224">Welch 2001 at Section 5.3.</p> <p data-bbox="499 1260 1961 1403">The Kalman filter requires both a model of the process dynamics and a model of the relationship between the process state and the available measurements. In part due to the simplicity of the SCAAT approach, we are able to use a simple position-velocity (PV) process model (Brown & Hwang, 1992). . . . We model the continuous change in the HiBall state with the simple differential equation</p>

Exhibit E-6

CLAIM 1	Welch 2001
	<div data-bbox="506 240 1268 764">$\frac{d}{dt}\tilde{x}(t) = \begin{bmatrix} 0 & 1 \\ 0 & 0 \end{bmatrix} \begin{bmatrix} x_p(t) \\ x_v(t) \end{bmatrix} + \begin{bmatrix} 0 \\ \mu \end{bmatrix} u(t), \quad (1)$<p>where $u(t)$ is a normally distributed white (in the frequency spectrum) scalar noise process, and the scalar μ represents the magnitude or spectral density of the noise. We use a similar model with a distinct noise process for each of the six pose elements. We determine the individual noise magnitudes using an offline simulation of the system and a nonlinear optimization strategy that seeks to minimize the variance between the estimated pose and a known motion path. (See section 6.2.2.).</p></div> <p data-bbox="506 805 846 836">Welch 2001 at Section 5.3.</p> <p data-bbox="506 873 1965 1019">The differential equation (1) represents a continuous integrated random walk, or an integrated Wiener or Brownian-motion process. Specifically, we model each component of the linear and angular HiBall velocities as a random walk, and then use these (assuming constant intermeasurement velocity) to estimate the HiBall pose at time $t + \delta t$ as follows:</p>

Exhibit E-6

CLAIM 1	Welch 2001
	<div data-bbox="730 266 1255 337" data-label="Equation-Block"> $\bar{x}(t + \delta t) = \begin{bmatrix} 1 & \delta t \\ 0 & 1 \end{bmatrix} \bar{x}(t) \quad (2)$ </div> <p data-bbox="520 380 1247 581">for each of the six pose elements. In addition to a relatively simple process model, the HiBall measurement model is relatively simple. For any ceiling LED (section 4.2) and HiBall view (section 4.1), the 2-D sensor measurement can be modeled as</p> <div data-bbox="793 623 1255 695" data-label="Equation-Block"> $\begin{bmatrix} u \\ v \end{bmatrix} = \begin{bmatrix} c_x/c_z \\ c_y/c_z \end{bmatrix} \quad (3)$ </div> <p data-bbox="520 737 600 769">where</p> <div data-bbox="739 812 1255 915" data-label="Equation-Block"> $\begin{bmatrix} c_x \\ c_y \\ c_z \end{bmatrix} = VR^T(\bar{l}_{xyz} - \bar{x}_{xyz}), \quad (4)$ </div> <p data-bbox="520 958 1247 1295">V is the camera viewing matrix from section 5.1, \bar{l}_{xyz} is the position of the LED in the world, \bar{x}_{xyz} is the position of the HiBall in the world, and R is a rotation matrix corresponding to the orientation of the HiBall in the world. In practice, we maintain the orientation of the HiBall as a combination of a global (external to the state) quaternion and a set of incremental angles as described by Welch (1996) and Welch and Bishop (1997).</p> <p data-bbox="504 1344 844 1377">Welch 2001 at Section 5.3.</p>

Exhibit E-6

CLAIM 1	Welch 2001
	<p>Because the measurement model (3) and (4) is non-linear, we use an extended Kalman filter, making use of the Jacobian of the nonlinear HiBall measurement model to transform the covariance of the Kalman filter. Welch 2001 at Section 5.3.</p> <p>Because the measurement model (3) and (4) is non-linear, we use an extended Kalman filter, making use of the Jacobian of the nonlinear HiBall measurement model to transform the covariance of the Kalman filter. Although this approach does not preserve the presumed Gaussian nature of the process, it has been used successfully in countless applications since the introduction of the (linear) Kalman filter. Based on observations of the statistics of the HiBall filter residuals, the approach also appears to work well for the HiBall. In fact, it is reasonable to expect that it would, as the speed of the SCAAT approach minimizes the distance (in state space) over which we use the Jacobian-based linear approximation. This is another example of the importance of the relationship shown in figure 12. Welch 2001 at Section 5.3.</p> <p>Once a particular view and LED have been chosen in this fashion, the CIB (section 4.3) is instructed to flash the LED and take a measurement as described in section 5.2. This single measurement is compared with a prediction obtained using equation (3), and the difference (or residual) is used to update the filter state and covariance matrices using the Kalman gain matrix. The Kalman gain is computed as a combination of the current filter covariance, the measurement noise variance (section 6.2.1), and the Jacobian of the measurement model. This recursive prediction-correction cycle continues in an ongoing fashion, a single constraint at a time. Welch 2001 at Section 5.3.</p> <p>Along with the benefit of simplicity and speed, the SCAAT approach offers the additional capability of being able to estimate the 3-D positions of the LEDs in the world concurrently with the pose of the HiBall, online, in real time. This capability is a tremendous benefit in terms of the accuracy and noise characteristics of the estimates.</p>

Exhibit E-6

CLAIM 1	Welch 2001
	<p data-bbox="520 248 1262 1109">The method we now use for autocalibration involves defining a distinct SCAAT Kalman filter for each LED. Specifically, for each LED, we maintain a state \bar{l} (estimate of the 3-D position) and a 3×3 Kalman filter covariance. At the beginning of each estimation cycle, we form an augmented state vector \hat{x} using the appropriate LED state and the current HiBall state: $\hat{x} = [\bar{x}^T, \bar{l}^T]^T$. Similarly, we augment the Kalman filter error covariance matrix with that of the LED filter. We then follow the normal steps outlined in section 5.3, with the result being that the LED portion of the filter state and covariance is updated in accordance with the measurement residual. At the end of the cycle, we extract the LED portions of the state and covariance from the augmented filter, and save them externally. The effect is that, as the system is being used, it continually refines its estimates of the LED positions, thereby continually improving its estimates of the HiBall pose. Again, for additional information, see Welch (1996) and Welch and Bishop (1997).</p> <p data-bbox="504 1157 846 1190">Welch 2001 at Section 5.4.</p> <p data-bbox="504 1227 1944 1369">The recursive nature of the Kalman filter (section 5.3) requires that the filter be initialized with a known state and corresponding covariance before steady-state operation can begin. Such an initialization (or acquisition) must take place prior to any tracking session, but also upon the (rare) occasion when the filter diverges and “loses lock” as a result of blocked sensor views, for example.</p> <p data-bbox="504 1373 846 1406">Welch 2001 at Section 5.5.</p>

Exhibit E-6


CLAIM 1	Welch 2001
	<p data-bbox="499 240 1955 418">The acquisition process is complicated by the fact that each LEPD sees a number of different widely separated views (section 4.1). Therefore, detecting an LED provides at best an ambiguous set of potential LED directions in HiBall coordinates. Moreover, before acquisition, no assumptions can be made to limit the search space of visible LEDs. As such, a relatively slow brute-force algorithm is used to acquire lock. Welch 2001 at Section 5.5.</p> <p data-bbox="499 456 1955 818">As a result of a mechanical design tradeoff, each sensor field of view is less than six degrees. The focal length is set by the size of the sensor housing, which is set by the diameter of the sensors themselves. Energetics is also a factor, limiting how small the lenses can be while maintaining sufficient light-collecting area. As a result of these design tradeoffs, even a momentary small error in the HiBall pose estimate can cause the recursive estimates to diverge and the system to lose lock after only a few LED sightings. And yet the system is quite robust. In practice, users can jump around, crawl on the floor, lean over, even wave their hands in front of the sensors, and the system does not lose lock. During one session, we were using the HiBall as a 3-D digitization probe, a Hi-Ball on the end of a pencil-shaped fiberglass wand (figure 14, left). We laid the probe down on a table at one point, and were amazed to later notice that it was still tracking, even though it was observing only three or four LEDs near the edge of the ceiling. We picked up the probe and continued using it, without it ever losing lock.</p> <div data-bbox="506 852 1129 1149"><p data-bbox="514 1109 646 1138">Figure 13.</p></div>

Exhibit E-6

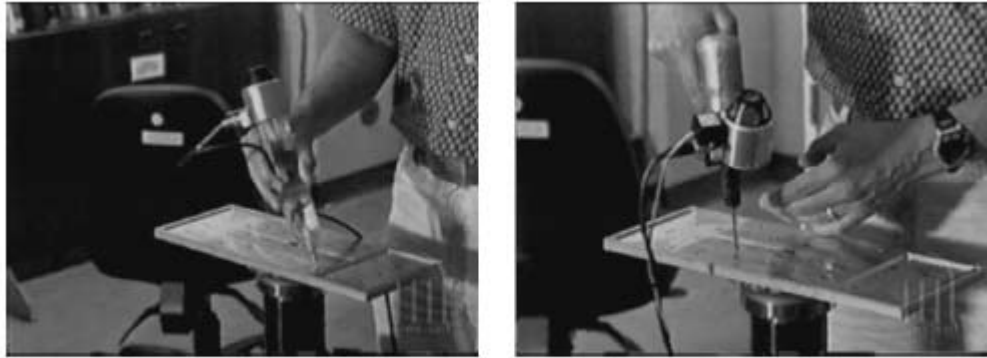
CLAIM 1	Welch 2001
	<div data-bbox="512 250 1493 605">  </div> <p data-bbox="512 625 646 657">Figure 14.</p> <p data-bbox="499 717 844 750">Welch 2001 at Section 6.1.</p> <p data-bbox="499 787 1961 1036">To make measurements of the noise when the HiBall is in motion, we rely on the assumption that almost all of the signal resulting from normal human motion is at frequencies below 2 Hz. We use a high-pass filter (Welch, 1967) on the pose estimates, and assume the output is noise. The resulting statistics are comparable to those made with the HiBall stationary, except at poses for which there are very few LEDs visible in only one or two views. In these poses, near the edge of the ceiling, the geometry of the constraints results in amplification of errors. For nearly all of the working volume of the tracker, the standard deviation of the noise on measurements while the HiBall is still or moving is about 0.2 mm and 0.03 deg.</p> <p data-bbox="499 1042 844 1075">Welch 2001 at Section 6.1.</p> <p data-bbox="499 1112 1961 1218">During the design of the HiBall system, we made substantial use of simulation, in some domains to a very detailed level. For example, Zemax (Focus Software, 1995) was used extensively in the design and optimization of the optical design, including the design of the filter glass lenses, and geometry of the optical-component layout.</p> <p data-bbox="499 1224 844 1256">Welch 2001 at Section 6.2.</p> <p data-bbox="499 1294 1961 1464">To produce realistic data for developing and tuning our algorithms, we collected several motion paths (sequences of pose estimates) from our first-generation electro-optical tracker (figure 3) at its 70 Hz maximum report rate. These paths were recorded from both naive users visiting our monthly “demo days” and from experienced users in our labs. . . . we filtered the raw path data with a noncausal zero-phase-shift, low-pass filter to eliminate energy above 2 Hz. The output of the low-pass filtering was then resampled at whatever rate we wanted to run the</p>

Exhibit E-6

CLAIM 1	Welch 2001
	<p>simulated tracker, usually 1,000 Hz. Welch 2001 at Section 6.2.</p> <p>The simulator reads camera models describing the 26 views, the sensor noise parameters, the LED positions and their expected error, and the motion path described above. Before beginning the simulation, the LED positions are perturbed from their ideal positions by adding normally distributed error to each axis. Then, for each simulated cycle of operation, the “true” poses are up- dated using the input motion path. Next, a view is chosen and a visible LED within that view is selected, and the image-plane coordinates of the LED on the chosen sensor are computed using the camera model for the view and the LED as described in section 5.3. These sensor coordinates are then perturbed based on the sensor noise model (section 6.2.1) using the distance and angle to the LED. These noise-corrupted sensor readings are then fed to the SCAAT filter to produce an up- dated position estimate. The position estimate is compared to the true position to produce a scalar error metric that is described next.</p> <p>Welch 2001 at Section 6.2.</p> <p>The error metric we used combines the error in pose in a way that relates to the effects of tracker error on a head-worn display user. We define a set of points arrayed around the user in a fixed configuration. We compute two sets of coordinates for these points: the true position using the true pose and their estimated position using the estimated pose. The error metric is then the sum of the distances between the true and estimated positions of these points. By adjusting the distance of the points from the user, we can control the relative importance of the orientation and the position error in the combined error metric. If the distance is small, then the position error is weighted most heavily; if the distance is large, then the orientation error is weighted most heavily. Our two error metrics for the entire run are the square root of the sum of the squares of all the distances, and the peak distance. Welch 2001 at Section 6.2.</p> <p><i>See also</i> Defendants’ Invalidity Contentions for further discussion.</p>

B. DEPENDENT CLAIM 2

CLAIM 2	Welch 2001
[2] The system of claim 1 wherein the sensor	At least under Plaintiffs’ apparent infringement theory, Welch 2001 discloses, either expressly or inherently, the system of claim 1 wherein the sensor subsystem includes one or more sensor modules, each providing an interface

Exhibit E-6

CLAIM 2	Welch 2001
<p>subsystem includes one or more sensor modules, each providing an interface for interacting with a corresponding set of one or more sensing elements.</p>	<p>for interacting with a corresponding set of one or more sensing elements. In the alternative, this element would be obvious over Welch 2001 in light of the other references disclosed in Defendants' Invalidity Contentions and/or the knowledge of one of ordinary skill in the art.</p> <p><i>See, e.g.:</i></p> <p>Thanks to significant improvements in hardware and software, this HiBall system offers unprecedented speed, resolution, accuracy, robustness, and flexibility. The bulky and heavy sensors and backpack of the previous system have been replaced by a small HiBall unit (figure 4, bottom). In addition, the precisely machined LED ceiling panels of the previous system have been replaced by looser-tolerance panels that are relatively inexpensive to make and simple to install (figure 4, top; figure 10). Finally, we are using an unusual Kalman-filter-based algorithm that generates very accurate pose estimates at a high rate with low latency, and that simultaneously self-calibrates the system.</p> <p>Welch 2001 at Section 1.3.</p> <p>As a result of these improvements, the HiBall Tracking System can generate more than 2,000 pose estimates per second, with less than 1 ms of latency, better than 0.5 mm and 0.03 deg. of absolute error and noise, everywhere in a 4.5 m x 8.5 m room (with more than two meters of height variation). The area can be expanded by adding more panels, or by using checker-board configurations that spread panels over a larger area. The weight of the user-worn HiBall is approximately 300 grams, making it lighter than one optical sensor in the 1991 system. Multiple HiBall units can be daisy-chained together for head or hand tracking, pose-aware input devices, or precise 3-D point digitization throughout the entire working volume.</p> <p>Welch 2001 at Section 1.3.</p>

Exhibit E-6


CLAIM 2	Welch 2001
	<div data-bbox="520 240 1060 1166">  <p data-bbox="520 1120 640 1153">Figure 4.</p> </div> <p data-bbox="520 1201 1963 1347">However, there are some significant advantages to the inside-looking-out approach for head tracking. By operating with sensors on the user rather than in the environment, the system can be scaled indefinitely. . . . The inside-looking-out configuration is also motivated by a desire to maximize sensitivity to changes in user pose.</p> <p data-bbox="520 1380 840 1412">Welch 2001 at Section 2.</p>

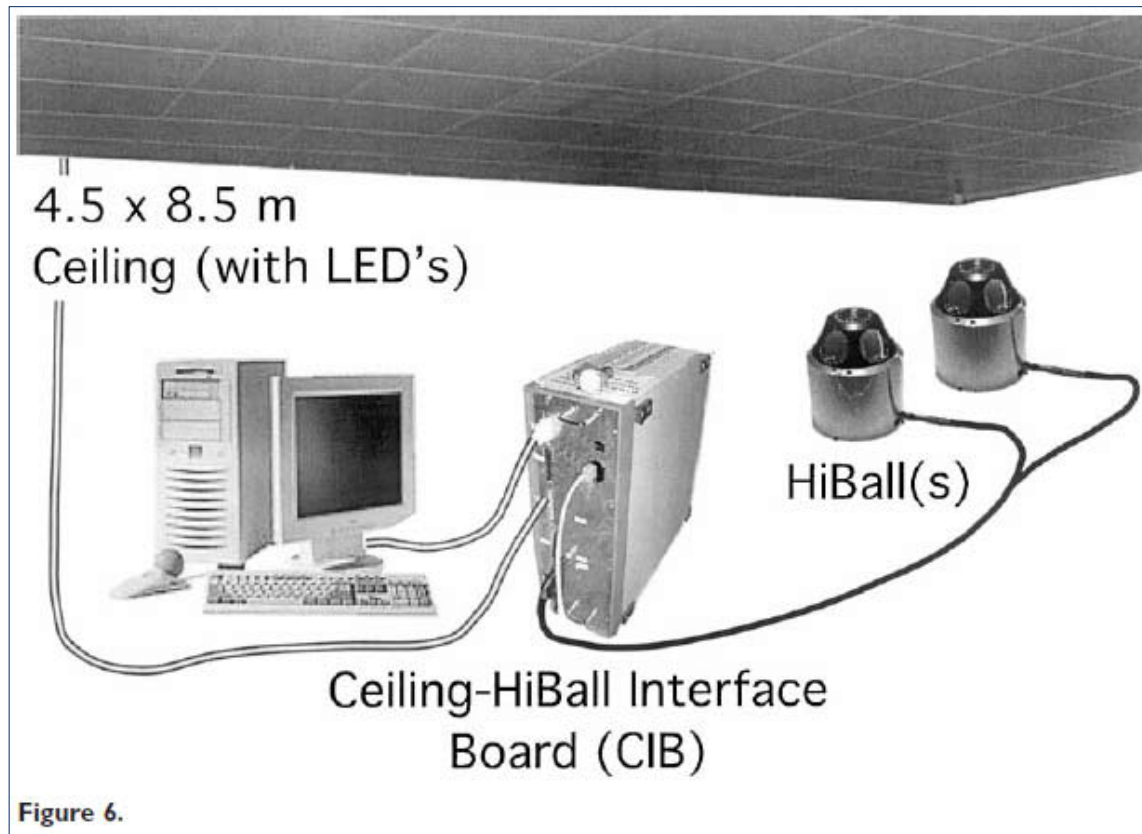
Exhibit E-6

CLAIM 2

Welch 2001

The HiBall Tracking System consists of three main components (figure 6). An outward-looking sensing unit we call the HiBall is fixed to each user to be tracked. The HiBall unit observes a subsystem of fixed-location infrared LEDs we call the Ceiling. Communication and synchronization between the host computer and these subsystems is coordinated by the Ceiling-HiBall Interface Board (CIB).

Welch 2001 at Section 3.



HiBall observes LEDs through multiple sensor-lens views that are distributed over a large solid angle. LEDs are sequentially flashed (one at a time) such that they are seen via a diverse set of views for each HiBall. Initial acquisition is performed using a brute-force search through LED space, but, once initial lock is made, the selection of LEDs to flash is tailored to the views of the active HiBall units. Pose estimates are maintained

Exhibit E-6

CLAIM 2	Welch 2001
	<p data-bbox="514 240 1961 380">using a Kalman-filter-based prediction-correction approach known as single-constraint-at-a-time (SCAAT) tracking. This technique has been extended to provide self-calibration of the ceiling, concurrent with HiBall tracking. Welch 2001 at Section 3.</p> <p data-bbox="514 418 1961 704">HiBall sensor unit was designed as a single, rigid, hollow ball having dodecahedral symmetry, with lenses in the upper six faces and LEPDs on the insides of the opposing six lower faces (figure 7). This immediately gives six primary “camera” views uniformly spaced by 57 deg. The views efficiently share the same internal air space and are rigid with respect to each other. In addition, light entering any lens sufficiently off-axis can be seen by a neighboring LEPD, giving rise to five secondary views through the top or central lens, and three secondary views through the five other lenses. Overall, this provides 26 fields of view that are used to sense widely separated groups of LEDs in the environment. Welch 2001 at Section 4.1.</p> <p data-bbox="514 743 1961 1062">The LEPDs themselves are not imaging devices; rather, they detect the centroid of the luminous flux incident on the detector. The x-position of the centroid determines the ratio of two output y-position determines the ratio of two other output currents. The total output current of each pair are commensurate and are proportional to the total incident flux. Consequently, focus is not an issue, so the simple fixed-focus lenses work well over a range of LED distances from about half a meter to infinity. The LEPDs and associated electronic components are mounted on a custom rigid-flex printed circuit board (figure 8). This arrangement makes efficient use of the internal HiBall volume while maintaining isolation between analog and digital circuitry, and increasing reliability by alleviating the need for intercomponent mechanical connectors. Welch 2001 at Section 4.1.</p> <p data-bbox="514 1101 1961 1419">Figure 9 shows the physical arrangement of the folded electronics in the HiBall. Each LEPD has four transimpedance amplifiers (shown together as one “Amp” in figure 9), the analog outputs of which are multiplexed with those of the other LEPDs, then sampled, held, and converted by four 16-bit Delta-Sigma analog-to-digital (A/D) converters. Multiple samples are integrated via an accumulator. The digitized LEPD data are organized into packets for communication back to the CIB. The packets also contain information to assist in error detection. The communication protocol is simple, and, while presently implemented by wire, the modulation scheme is amenable to a wireless implementation. The present wired implementation allows multiple HiBall units to be daisy-chained, so a single cable can support a user with multiple HiBall units. Welch 2001 at Section 4.1.</p>

Exhibit E-6

CLAIM 2	Welch 2001
	<div data-bbox="520 240 1528 1003"> <p>Figure 9.</p> </div> <p>As presently implemented, the infrared LEDs are packaged in 61 cm square panels to fit a standard false-ceiling grid (figure 10, top). Each panel uses five printed circuit boards: a main controller board and four identical transverse-mounted strips (bottom). Each strip is populated with eight LEDs for a total of 32 LEDs per panel. We mount the assembly on top of a metal panel such that the LEDs protrude through 32 corresponding holes. The design results in a ceiling with a rectangular LED pattern with periods of 7.6 cm and 15.2 cm. This spacing is used for the initial estimates of the LED positions in the lab; then, during normal operation, the SCAAT algorithm continually refines the LED position estimates (section 5.4). The SCAAT autocalibration not only relaxes design and installation constraints, but provides greater precision in the face of initial and ongoing uncertainty in the ceiling structure.</p> <p>Welch 2001 at Section 4.2.</p>

Exhibit E-6

CLAIM 2	Welch 2001
	<div data-bbox="527 250 974 683" data-label="Image"> </div> <div data-bbox="527 719 974 1052" data-label="Image"> </div> <div data-bbox="525 1066 651 1102" data-label="Caption"> <p>Figure 7.</p> </div> <div data-bbox="504 1146 1988 1367" data-label="Text"> <p>The Ceiling-HiBall Interface Board (CIB) (figure 11) provides communication and synchronization between a host personal computer, the HiBall (section 4.1), and the ceiling (section 4.2). The CIB has four ceiling ports allowing interleaving of ceiling panels for up to four simultaneous LED flashes and/or higher ceiling bandwidth. (The ceiling bandwidth is inherently limited by LED power restrictions as described in section 4.2, but this can be increased by spatially multiplexing the ceiling panels.) The CIB has two tether interfaces that can communicate with up to four daisy chained HiBall units. The full-duplex communication with the</p> </div>

Exhibit E-6

CLAIM 2	Welch 2001
	<p data-bbox="514 240 1963 310">HiBall units uses a modulation scheme (BPSK) allowing future wireless operation. The interface from the CIB to the host PC is the stable IEEE1284C extended parallel port (EPP) standard.</p> <p data-bbox="514 345 1963 488">The CIB comprises analog drive and receive components as well as digital logic components. The digital components implement store and forward in both directions and synchronize the timing of the LED “on” interval within the HiBall dark-light-dark intervals (section 5.2). The protocol supports full-duplex flow control. The data are arranged into packets that incorporate error detection.</p> <p data-bbox="514 524 861 553">Welch 2001 at Section 4.3.</p> <p data-bbox="514 589 1963 732">Upon receiving a command from the CIB (section 4.3), which is synchronized with a CIB command to the ceiling, the HiBall selects the specified LED and performs three measurements, one before the LED flashes, one during the LED flash, and one after the LED flash. Known as “dark-light-dark,” this technique is used to subtract out DC bias, low-frequency noise, and background light from the LED signal.</p> <p data-bbox="514 740 1963 810">We then convert the measured sensor coordinates to “ideal” coordinates using the calibration tables described in section 5.1.</p> <p data-bbox="514 846 1963 1170">In addition, during runtime we attempt to maximize the signal-to-noise ratio of the measurement with an automatic gain-control scheme. For each LED, we store a target signal strength factor. We compute the LED current and number of integrations (of successive accumulated A/D samples) by dividing this strength factor by the square of the distance to the LED, estimated from the current position estimate. After a reading, we look at the strength of the actual measurement. If it is larger than expected, we reduce the gain; if it is less than expected, we increase the gain. The increase and decrease are implemented as online averages with scaling such that the gain factor decreases rapidly (to avoid overflow) and increases slowly. Finally, we use the measured signal strength to estimate the noise on the signal using (Chi, 1995), and then use this as the measurement noise estimate for the Kalman filter (section 5.3).</p> <p data-bbox="514 1206 861 1235">Welch 2001 at Section 5.2.</p> <p data-bbox="514 1271 1963 1383">The online measurements (section 5.2) are used to estimate the pose of the HiBall during operation. The 1991 system collected a group of diverse measurements for a variety of LEDs and sensors, and then used a method of simultaneous nonlinear equations called collinearity (Azuma & Ward, 1991) to estimate the</p>

Exhibit E-6

CLAIM 2	Welch 2001
	<p>pose of the sensor fixture shown in figure 3 (bottom). Welch 2001 at Section 5.3.</p> <p>In contrast, the approach we use with the new HiBall system produces tracker reports as each new measurement is made, rather than waiting to form a complete collection of observations. Because single measurements under constrain the mathematical solution, we refer to the approach as single-constraint-at-a-time (SCAAT) tracking (Welch, 1996; Welch & Bishop, 1997). The key is that the single measurements provide some information about the HiBall's state, and thus can be used to incrementally improve a previous estimate. We intentionally fuse each individual “insufficient” measurement immediately as it is obtained. With this approach, we are able to generate estimates more frequently, with less latency, and with improved accuracy, and we are able to estimate the LED positions online concurrently while tracking the HiBall (section 5.4). Welch 2001 at Section 5.3.</p> <p>We use a Kalman filter (Kalman, 1960) to fuse the measurements into an estimate of the HiBall state x (the pose of the HiBall). We use the Kalman filter—a minimum-variance stochastic estimator—both because the sensor measurement noise and the typical user-motion dynamics can be modeled as normally distributed random processes, and because we want an efficient online method of estimation. Welch 2001 at Section 5.3.</p> <p>The Kalman filter has been used previously to address similar or related problems. . . . A relevant example of a Kalman filter used for sensor fusion in a wide-area tracking system is given in Foxlin et al. (1998), which describes a hybrid inertial-acoustic system that is commercially available today (Intersense, 2000). Welch 2001 at Section 5.3.</p> <p>[O]ne key benefit warrants discussion here. There is a direct relationship between the complexity of the estimation algorithm, the corresponding speed (execution time per estimation cycle), and the change in HiBall pose between estimation cycles (figure 12). As the algorithmic complexity increases, the execution time increases, which allows for significant nonlinear HiBall motion between estimation cycles, which in turn implies the need for a more complex estimation algorithm. Welch 2001 at Section 5.3.</p>

Exhibit E-6


CLAIM 2	Welch 2001
	<div data-bbox="520 240 1140 933">  <p data-bbox="531 898 661 925">Figure 12.</p> </div> <p data-bbox="514 971 1957 1222"> The SCAAT approach, on the other hand, is an attempt to reverse this cycle. Because we intentionally use a single constraint per estimate, the algorithmic complexity is drastically reduced, which reduces the execution time, and hence the amount of motion between estimation cycles. Because the amount of motion is limited, we are able to use a simple dynamic (process) model in the Kalman filter, which further simplifies the computations. In short, the simplicity of the approach means that it can run very fast, which means it can produce estimates very rapidly, with low noise. Welch 2001 at Section 5.3. </p> <p data-bbox="514 1258 1957 1437"> At each estimation cycle, the next of the 26 possible views is chosen randomly. Four points corresponding to the corners of the LEPD sensor associated with that view are projected into the world using the 3 3 4 viewing matrix for that view, along with the current estimates of the HiBall pose. This projection, which is the inverse of the measurement relationship described above, results in four rays extending from the sensor into the world. The intersection of these rays and the approximate plane of the ceiling determines a 2-D bounding box on the ceiling, </p>

Exhibit E-6

CLAIM 2	Welch 2001
	<p>within which are the candidate LEDs for the current view. One of the candidate LEDs is then chosen in a least-recently-used fashion to ensure a diversity of constraints.</p> <p>Once a particular view and LED have been chosen in this fashion, the CIB (section 4.3) is instructed to flash the LED and take a measurement as described in section 5.2. This single measurement is compared with a prediction obtained using equation (3), and the difference (or residual) is used to update the filter state and covariance matrices using the Kalman gain matrix. The Kalman gain is computed as a combination of the current filter covariance, the measurement noise variance (section 6.2.1), and the Jacobian of the measurement model. This recursive prediction-correction cycle continues in an ongoing fashion, a single constraint at a time.</p> <p>Welch 2001 at Section 5.3.</p> <p>for each of the six pose elements. In addition to a relatively simple process model, the HiBall measurement model is relatively simple. For any ceiling LED (section 4.2) and HiBall view (section 4.1), the 2-D sensor measurement can be modeled as</p> $\begin{bmatrix} u \\ v \end{bmatrix} = \begin{bmatrix} c_x/c_z \\ c_y/c_z \end{bmatrix} \quad (3)$ <p>where</p> $\begin{bmatrix} c_x \\ c_y \\ c_z \end{bmatrix} = VR^T(\bar{l}_{xyz} - \bar{x}_{xyz}), \quad (4)$ <p>V is the camera viewing matrix from section 5.1, \bar{l}_{xyz} is the position of the LED in the world, \bar{x}_{xyz} is the position of the HiBall in the world, and R is a rotation matrix corresponding to the orientation of the HiBall in the world. In practice, we maintain the orientation of the HiBall as a combination of a global (external to the state) quaternion and a set of incremental angles as described by Welch (1996) and Welch and Bishop (1997).</p> <p>Welch 2001 at Section 5.3.</p>

Exhibit E-6

CLAIM 2	Welch 2001
	<p>The method we now use for autocalibration involves defining a distinct SCAAT Kalman filter for each LED. Specifically, for each LED, we maintain a state \bar{l} (estimate of the 3-D position) and a 3 x 3 Kalman filter covariance. At the beginning of each estimation cycle, we form an augmented state vector \bar{x} using the appropriate LED state and the current HiBall state: $\bar{x} = [\bar{x}^T, \bar{l}^T]^T$. Similarly, we augment the Kalman filter error covariance matrix with that of the LED filter. We then follow the normal steps outlined in section 5.3, with the result being that the LED portion of the filter state and covariance is updated in accordance with the measurement residual. At the end of the cycle, we extract the LED portions of the state and covariance from the augmented filter, and save them externally. The effect is that, as the system is being used, it continually refines its estimates of the LED positions, thereby continually improving its estimates of the HiBall pose. Again, for additional information, see Welch (1996) and Welch and Bishop (1997).</p> <p>Welch 2001 at Section 5.4.</p> <p>During the design of the HiBall system, we made substantial use of simulation, in some domains to a very detailed level. For example, Zemax (Focus Software, 1995) was used extensively in the design and optimization of the optical design, including the design of the filter glass lenses, and geometry of the optical-component layout.</p> <p>Welch 2001 at Section 6.2.</p> <p><i>See Disclosures with respect to Claim 1, supra; see also Defendants' Invalidity Contentions for further discussion.</i></p>

C. DEPENDENT CLAIM 3

CLAIM 3	Welch 2001
<p>[3] The system of claim 2 wherein the interface enables the sensor module to perform computations independently of an</p>	<p>At least under Plaintiffs' apparent infringement theory, Welch 2001 discloses, either expressly or inherently, the system of claim 2 wherein the interface enables the sensor module to perform computations independently of an implementation of the estimation subsystem. In the alternative, this element would be obvious over Welch 2001 in light of the other references disclosed in Defendants' Invalidity Contentions and/or the knowledge of one of ordinary skill in the art.</p> <p><i>See, e.g.:</i></p>

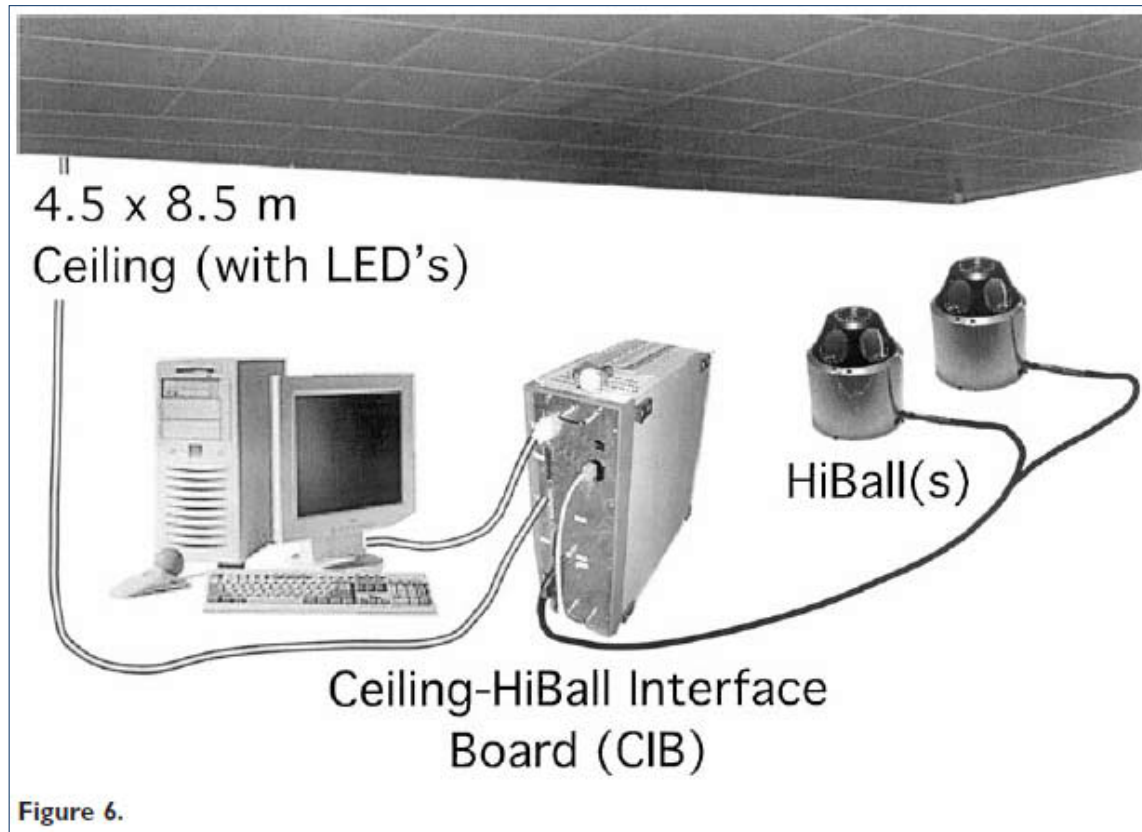
Exhibit E-6

CLAIM 3	Welch 2001
implementation of the estimation subsystem.	<p>Thanks to significant improvements in hardware and software, this HiBall system offers unprecedented speed, resolution, accuracy, robustness, and flexibility. The bulky and heavy sensors and backpack of the previous system have been replaced by a small HiBall unit (figure 4, bottom). In addition, the precisely machined LED ceiling panels of the previous system have been replaced by looser-tolerance panels that are relatively inexpensive to make and simple to install (figure 4, top; figure 10). Finally, we are using an unusual Kalman-filter-based algorithm that generates very accurate pose estimates at a high rate with low latency, and that simultaneously self-calibrates the system.</p> <p>Welch 2001 at Section 1.3.</p> <p>The HiBall Tracking System consists of three main components (figure 6). An outward-looking sensing unit we call the HiBall is fixed to each user to be tracked. The HiBall unit observes a subsystem of fixed-location infrared LEDs we call the Ceiling. Communication and synchronization between the host computer and these subsystems is coordinated by the Ceiling-HiBall Interface Board (CIB).</p> <p>Welch 2001 at Section 3.</p>

Exhibit E-6

CLAIM 3

Welch 2001



The original electro-optical tracker (figure 3, bottom) used independently housed lateral-effect photodiode units (LEPDs) attached to a lightweight tubular framework. As it turns out, the mechanical framework would flex (distort) during use, contributing to estimation errors. In part to address this problem, the HiBall sensor unit was designed as a single, rigid, hollow ball having dodecahedral symmetry, with lenses in the upper six faces and LEPDs on the insides of the opposing six lower faces (figure 7). This immediately gives six primary “camera” views uniformly spaced by 57 deg. The views efficiently share the same internal air space and are rigid with respect to each other. In addition, light entering any lens sufficiently off-axis can be seen by a neighboring LEPD, giving rise to five secondary views through the top or central lens, and three secondary views through the five other lenses. Overall, this provides 26 fields of view that are used to sense widely separated groups of LEDs

Exhibit E-6

CLAIM 3	Welch 2001
	<p>in the environment. Although the extra views complicate the initialization of the Kalman filter as described in section 5.5, they turn out to be of great benefit during steady-state tracking by effectively increasing the overall HiBall field of view without sacrificing optical-sensor resolution.</p> <p>Welch 2001 at Section 4.1</p> <p>Figure 9 shows the physical arrangement of the folded electronics in the HiBall. Each LEPD has four transimpedance amplifiers (shown together as one “Amp” in figure 9), the analog outputs of which are multiplexed with those of the other LEPDs, then sampled, held, and converted by four 16-bit Delta-Sigma analog-to-digital (A/D) converters. Multiple samples are integrated via an accumulator. The digitized LEPD data are organized into packets for communication back to the CIB. The packets also contain information to assist in error detection. The communication protocol is simple, and, while presently implemented by wire, the modulation scheme is amenable to a wireless implementation.</p> <p>Welch 2001 at Section 4.1.</p> <p>The CIB comprises analog drive and receive components as well as digital logic components. The digital components implement store and forward in both directions and synchronize the timing of the LED “on” interval within the HiBall dark-light-dark intervals (section 5.2). The protocol supports full-duplex flow control. The data are arranged into packets that incorporate error detection.</p> <p>Welch 2001 at Section 4.3.</p>

Exhibit E-6

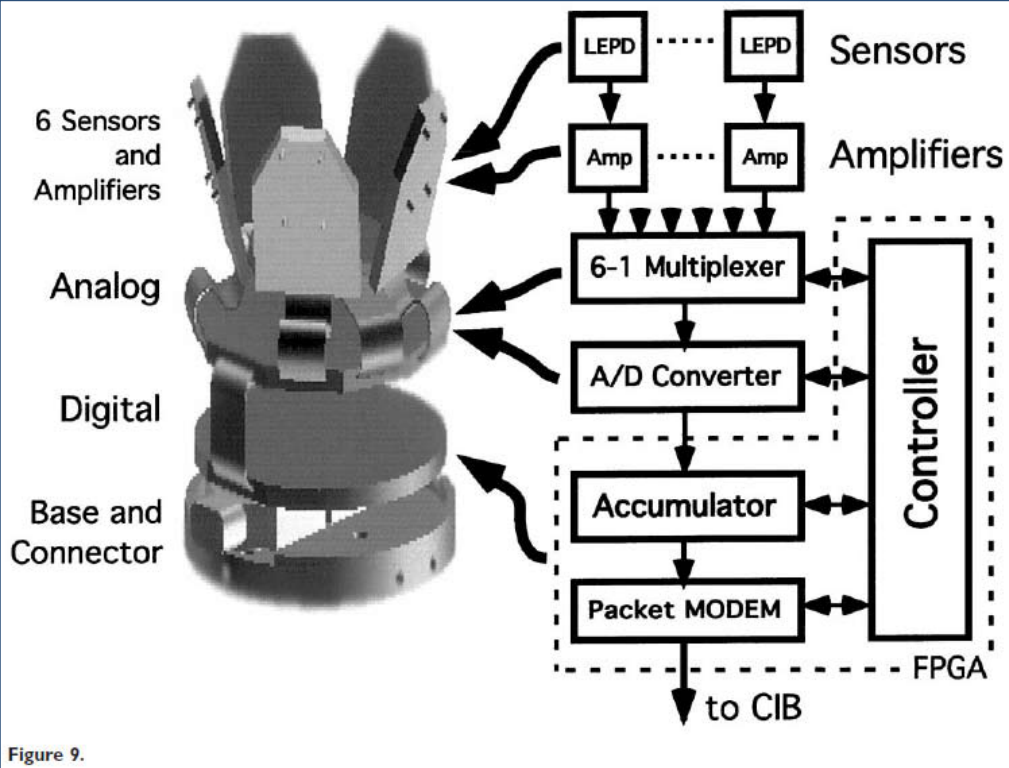
CLAIM 3	Welch 2001
	 <p>Figure 9.</p> <p>The online measurements (section 5.2) are used to estimate the pose of the HiBall during operation. The 1991 system collected a group of diverse measurements for a variety of LEDs and sensors, and then used a method of simultaneous nonlinear equations called collinearity (Azuma & Ward, 1991) to estimate the pose of the sensor fixture shown in figure 3 (bottom).</p> <p>Welch 2001 at Section 5.3.</p> <p>In contrast, the approach we use with the new HiBall system produces tracker reports as each new measurement is made, rather than waiting to form a complete collection of observations. Because single measurements under constrain the mathematical solution, we refer to the approach as single-constraint-at-a-time (SCAAT) tracking (Welch, 1996; Welch & Bishop, 1997). The key is that the single measurements provide some information about the HiBall's state, and thus can be used to incrementally improve a</p>

Exhibit E-6

CLAIM 3	Welch 2001
	<p>previous estimate. We intentionally fuse each individual “insufficient” measurement immediately as it is obtained. With this approach, we are able to generate estimates more frequently, with less latency, and with improved accuracy, and we are able to estimate the LED positions online concurrently while tracking the HiBall (section 5.4). Welch 2001 at Section 5.3.</p> <p>We use a Kalman filter (Kalman, 1960) to fuse the measurements into an estimate of the HiBall state x (the pose of the HiBall). We use the Kalman filter—a minimum-variance stochastic estimator—both because the sensor measurement noise and the typical user-motion dynamics can be modeled as normally distributed random processes, and because we want an efficient online method of estimation. Welch 2001 at Section 5.3.</p> <p>The Kalman filter has been used previously to address similar or related problems. . . . A relevant example of a Kalman filter used for sensor fusion in a wide-area tracking system is given in Foxlin et al. (1998), which describes a hybrid inertial-acoustic system that is commercially available today (Intersense, 2000). Welch 2001 at Section 5.3.</p> <p>[O]ne key benefit warrants discussion here. There is a direct relationship between the complexity of the estimation algorithm, the corresponding speed (execution time per estimation cycle), and the change in HiBall pose between estimation cycles (figure 12). As the algorithmic complexity increases, the execution time increases, which allows for significant nonlinear HiBall motion between estimation cycles, which in turn implies the need for a more complex estimation algorithm. Welch 2001 at Section 5.3.</p>

Exhibit E-6


CLAIM 3	Welch 2001
	<div data-bbox="520 240 1140 933">  <p data-bbox="531 898 661 925">Figure 12.</p> </div> <p data-bbox="514 971 1957 1222"> The SCAAT approach, on the other hand, is an attempt to reverse this cycle. Because we intentionally use a single constraint per estimate, the algorithmic complexity is drastically reduced, which reduces the execution time, and hence the amount of motion between estimation cycles. Because the amount of motion is limited, we are able to use a simple dynamic (process) model in the Kalman filter, which further simplifies the computations. In short, the simplicity of the approach means that it can run very fast, which means it can produce estimates very rapidly, with low noise. Welch 2001 at Section 5.3. </p> <p data-bbox="514 1258 1946 1401"> The Kalman filter requires both a model of the process dynamics and a model of the relationship between the process state and the available measurements. In part due to the simplicity of the SCAAT approach, we are able to use a simple position-velocity (PV) process model (Brown & Hwang, 1992). . . . We model the continuous change in the HiBall state with the simple differential equation </p>

Exhibit E-6

CLAIM 3	Welch 2001
	<div data-bbox="520 240 1283 764">$\frac{d}{dt}\bar{x}(t) = \begin{bmatrix} 0 & 1 \\ 0 & 0 \end{bmatrix} \begin{bmatrix} x_p(t) \\ x_v(t) \end{bmatrix} + \begin{bmatrix} 0 \\ \mu \end{bmatrix} u(t), \quad (1)$<p>where $u(t)$ is a normally distributed white (in the frequency spectrum) scalar noise process, and the scalar μ represents the magnitude or spectral density of the noise. We use a similar model with a distinct noise process for each of the six pose elements. We determine the individual noise magnitudes using an offline simulation of the system and a nonlinear optimization strategy that seeks to minimize the variance between the estimated pose and a known motion path. (See section 6.2.2.).</p></div> <p data-bbox="520 805 861 837">Welch 2001 at Section 5.3.</p> <p data-bbox="520 873 1965 1019">The differential equation (1) represents a continuous integrated random walk, or an integrated Wiener or Brownian-motion process. Specifically, we model each component of the linear and angular HiBall velocities as a random walk, and then use these (assuming constant intermeasurement velocity) to estimate the HiBall pose at time $t + \delta t$ as follows:</p>

Exhibit E-6

CLAIM 3	Welch 2001
	<div data-bbox="743 269 1272 341" data-label="Equation-Block"> $\bar{x}(t + \delta t) = \begin{bmatrix} 1 & \delta t \\ 0 & 1 \end{bmatrix} \bar{x}(t) \quad (2)$ </div> <div data-bbox="533 380 1264 581" data-label="Text"> <p>for each of the six pose elements. In addition to a relatively simple process model, the HiBall measurement model is relatively simple. For any ceiling LED (section 4.2) and HiBall view (section 4.1), the 2-D sensor measurement can be modeled as</p> </div> <div data-bbox="802 626 1272 698" data-label="Equation-Block"> $\begin{bmatrix} u \\ v \end{bmatrix} = \begin{bmatrix} c_x/c_z \\ c_y/c_z \end{bmatrix} \quad (3)$ </div> <div data-bbox="533 737 617 771" data-label="Text"> <p>where</p> </div> <div data-bbox="743 816 1272 919" data-label="Equation-Block"> $\begin{bmatrix} c_x \\ c_y \\ c_z \end{bmatrix} = VR^T(\bar{l}_{xyz} - \bar{x}_{xyz}), \quad (4)$ </div> <div data-bbox="533 958 1272 1295" data-label="Text"> <p>V is the camera viewing matrix from section 5.1, \bar{l}_{xyz} is the position of the LED in the world, \bar{x}_{xyz} is the position of the HiBall in the world, and R is a rotation matrix corresponding to the orientation of the HiBall in the world. In practice, we maintain the orientation of the HiBall as a combination of a global (external to the state) quaternion and a set of incremental angles as described by Welch (1996) and Welch and Bishop (1997).</p> </div> <div data-bbox="512 1341 861 1377" data-label="Text"> <p>Welch 2001 at Section 5.3.</p> </div>

Exhibit E-6

CLAIM 3	Welch 2001
	<p>Because the measurement model (3) and (4) is non-linear, we use an extended Kalman filter, making use of the Jacobian of the nonlinear HiBall measurement model to transform the covariance of the Kalman filter. Welch 2001 at Section 5.3.</p> <p>Along with the benefit of simplicity and speed, the SCAAT approach offers the additional capability of being able to estimate the 3-D positions of the LEDs in the world concurrently with the pose of the HiBall, online, in real time. This capability is a tremendous benefit in terms of the accuracy and noise characteristics of the estimates.</p>

Exhibit E-6

CLAIM 3	Welch 2001
	<div data-bbox="520 240 1283 1120"><p>The method we now use for autocalibration involves defining a distinct SCAAT Kalman filter for each LED. Specifically, for each LED, we maintain a state \bar{l} (estimate of the 3-D position) and a 3×3 Kalman filter covariance. At the beginning of each estimation cycle, we form an augmented state vector \hat{x} using the appropriate LED state and the current HiBall state: $\hat{x} = [\bar{x}^T, \bar{l}^T]^T$. Similarly, we augment the Kalman filter error covariance matrix with that of the LED filter. We then follow the normal steps outlined in section 5.3, with the result being that the LED portion of the filter state and covariance is updated in accordance with the measurement residual. At the end of the cycle, we extract the LED portions of the state and covariance from the augmented filter, and save them externally. The effect is that, as the system is being used, it continually refines its estimates of the LED positions, thereby continually improving its estimates of the HiBall pose. Again, for additional information, see Welch (1996) and Welch and Bishop (1997).</p></div> <p data-bbox="520 1159 861 1190">Welch 2001 at Section 5.4.</p> <div data-bbox="520 1229 1959 1370"><p>The recursive nature of the Kalman filter (section 5.3) requires that the filter be initialized with a known state and corresponding covariance before steady-state operation can begin. Such an initialization (or acquisition) must take place prior to any tracking session, but also upon the (rare) occasion when the filter diverges and “loses lock” as a result of blocked sensor views, for example.</p></div> <p data-bbox="520 1377 861 1408">Welch 2001 at Section 5.5.</p>

Exhibit E-6

CLAIM 3	Welch 2001
	<i>See</i> Disclosures with respect to Claim 2, <i>supra</i> ; <i>see also</i> Defendants' Invalidity Contentions for further discussion.

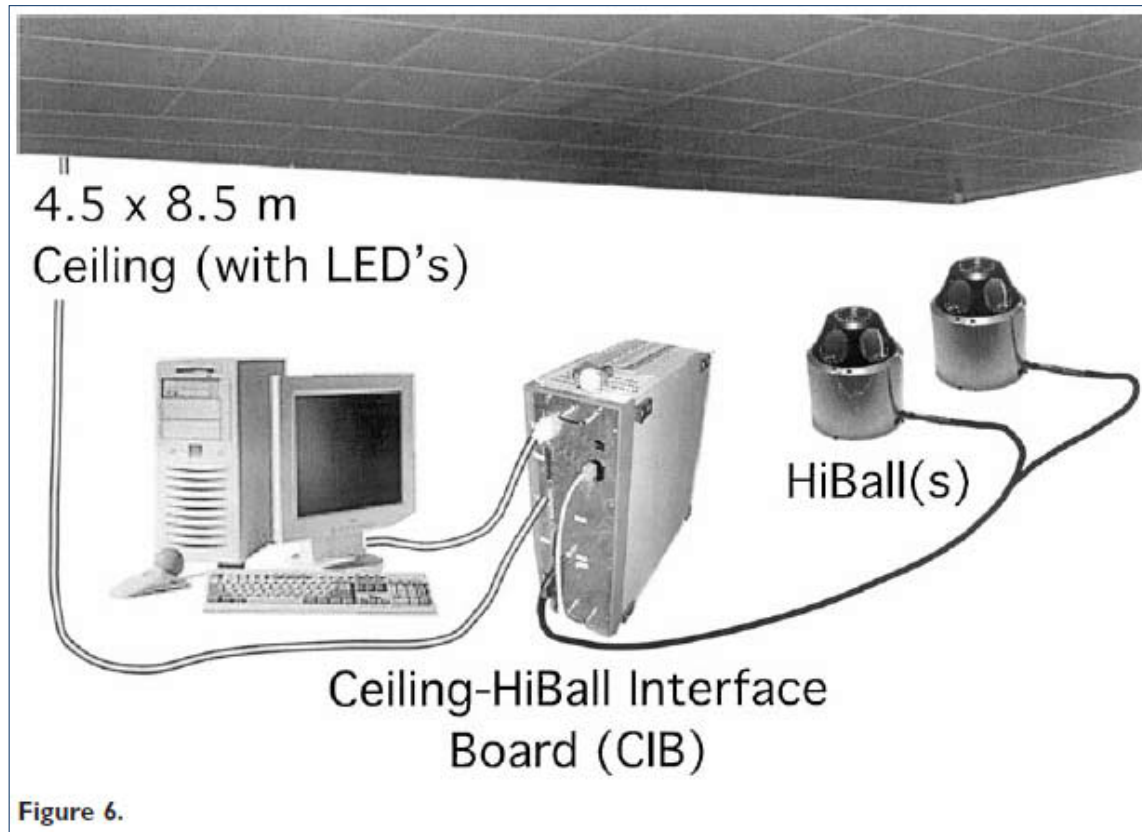
D. DEPENDENT CLAIM 4

CLAIM 4	Welch 2001
[4] The system of claim 2 wherein the interface enables the estimation subsystem to perform computations independently of an implementation of the sensor modules.	<p>At least under Plaintiffs' apparent infringement theory, Welch 2001 discloses, either expressly or inherently, the system of claim 2 wherein the interface enables the estimation subsystem to perform computations independently of an implementation of the sensor modules. In the alternative, this element would be obvious over Welch 2001 in light of the other references disclosed in Defendants' Invalidity Contentions and/or the knowledge of one of ordinary skill in the art.</p> <p><i>See, e.g.:</i></p> <p>Thanks to significant improvements in hardware and software, this HiBall system offers unprecedented speed, resolution, accuracy, robustness, and flexibility. The bulky and heavy sensors and backpack of the previous system have been replaced by a small HiBall unit (figure 4, bottom). In addition, the precisely machined LED ceiling panels of the previous system have been replaced by looser-tolerance panels that are relatively inexpensive to make and simple to install (figure 4, top; figure 10). Finally, we are using an unusual Kalman-filter-based algorithm that generates very accurate pose estimates at a high rate with low latency, and that simultaneously self-calibrates the system.</p> <p>Welch 2001 at Section 1.3.</p> <p>The HiBall Tracking System consists of three main components (figure 6). An outward-looking sensing unit we call the HiBall is fixed to each user to be tracked. The HiBall unit observes a subsystem of fixed-location infrared LEDs we call the Ceiling. Communication and synchronization between the host computer and these subsystems is coordinated by the Ceiling-HiBall Interface Board (CIB).</p> <p>Welch 2001 at Section 3.</p>

Exhibit E-6

CLAIM 4

Welch 2001



The original electro-optical tracker (figure 3, bottom) used independently housed lateral-effect photodiode units (LEPDs) attached to a lightweight tubular framework. As it turns out, the mechanical framework would flex (distort) during use, contributing to estimation errors. In part to address this problem, the HiBall sensor unit was designed as a single, rigid, hollow ball having dodecahedral symmetry, with lenses in the upper six faces and LEPDs on the insides of the opposing six lower faces (figure 7). This immediately gives six primary “camera” views uniformly spaced by 57 deg. The views efficiently share the same internal air space and are rigid with respect to each other. In addition, light entering any lens sufficiently off-axis can be seen by a neighboring LEPD, giving rise to five secondary views through the top or central lens, and three secondary views through the five other lenses. Overall, this provides 26 fields of view that are used to sense widely separated groups of LEDs

Exhibit E-6

CLAIM 4	Welch 2001
	<p>in the environment. Although the extra views complicate the initialization of the Kalman filter as described in section 5.5, they turn out to be of great benefit during steady-state tracking by effectively increasing the overall HiBall field of view without sacrificing optical-sensor resolution.</p> <p>Welch 2001 at Section 4.1</p> <p>Figure 9 shows the physical arrangement of the folded electronics in the HiBall. Each LEPD has four transimpedance amplifiers (shown together as one “Amp” in figure 9), the analog outputs of which are multiplexed with those of the other LEPDs, then sampled, held, and converted by four 16-bit Delta-Sigma analog-to-digital (A/D) converters. Multiple samples are integrated via an accumulator. The digitized LEPD data are organized into packets for communication back to the CIB. The packets also contain information to assist in error detection. The communication protocol is simple, and, while presently implemented by wire, the modulation scheme is amenable to a wireless implementation.</p> <p>Welch 2001 at Section 4.1.</p> <p>The CIB comprises analog drive and receive components as well as digital logic components. The digital components implement store and forward in both directions and synchronize the timing of the LED “on” interval within the HiBall dark-light-dark intervals (section 5.2). The protocol supports full-duplex flow control. The data are arranged into packets that incorporate error detection.</p> <p>Welch 2001 at Section 4.3.</p>

Exhibit E-6

CLAIM 4	Welch 2001
	<div data-bbox="520 240 1528 1003"> <p>Figure 9.</p> </div> <p>The online measurements (section 5.2) are used to estimate the pose of the HiBall during operation. The 1991 system collected a group of diverse measurements for a variety of LEDs and sensors, and then used a method of simultaneous nonlinear equations called collinearity (Azuma & Ward, 1991) to estimate the pose of the sensor fixture shown in figure 3 (bottom).</p> <p>Welch 2001 at Section 5.3.</p> <p>In contrast, the approach we use with the new HiBall system produces tracker reports as each new measurement is made, rather than waiting to form a complete collection of observations. Because single measurements under constrain the mathematical solution, we refer to the approach as single-constraint-at-a-time (SCAAT) tracking (Welch, 1996; Welch & Bishop, 1997). The key is that the single measurements provide some information about the HiBall's state, and thus can be used to incrementally improve a</p>

Exhibit E-6

CLAIM 4	Welch 2001
	<p>previous estimate. We intentionally fuse each individual “insufficient” measurement immediately as it is obtained. With this approach, we are able to generate estimates more frequently, with less latency, and with improved accuracy, and we are able to estimate the LED positions online concurrently while tracking the HiBall (section 5.4). Welch 2001 at Section 5.3.</p> <p>We use a Kalman filter (Kalman, 1960) to fuse the measurements into an estimate of the HiBall state x (the pose of the HiBall). We use the Kalman filter—a minimum-variance stochastic estimator—both because the sensor measurement noise and the typical user-motion dynamics can be modeled as normally distributed random processes, and because we want an efficient online method of estimation. Welch 2001 at Section 5.3.</p> <p>The Kalman filter has been used previously to address similar or related problems. . . . A relevant example of a Kalman filter used for sensor fusion in a wide-area tracking system is given in Foxlin et al. (1998), which describes a hybrid inertial-acoustic system that is commercially available today (Intersense, 2000). Welch 2001 at Section 5.3.</p> <p>[O]ne key benefit warrants discussion here. There is a direct relationship between the complexity of the estimation algorithm, the corresponding speed (execution time per estimation cycle), and the change in HiBall pose between estimation cycles (figure 12). As the algorithmic complexity increases, the execution time increases, which allows for significant nonlinear HiBall motion between estimation cycles, which in turn implies the need for a more complex estimation algorithm. Welch 2001 at Section 5.3.</p>

Exhibit E-6


CLAIM 4	Welch 2001
	<div data-bbox="520 240 1140 933">  <p data-bbox="531 898 661 925">Figure 12.</p> </div> <p data-bbox="514 971 1957 1222"> The SCAAT approach, on the other hand, is an attempt to reverse this cycle. Because we intentionally use a single constraint per estimate, the algorithmic complexity is drastically reduced, which reduces the execution time, and hence the amount of motion between estimation cycles. Because the amount of motion is limited, we are able to use a simple dynamic (process) model in the Kalman filter, which further simplifies the computations. In short, the simplicity of the approach means that it can run very fast, which means it can produce estimates very rapidly, with low noise. Welch 2001 at Section 5.3. </p> <p data-bbox="514 1258 1946 1401"> The Kalman filter requires both a model of the process dynamics and a model of the relationship between the process state and the available measurements. In part due to the simplicity of the SCAAT approach, we are able to use a simple position-velocity (PV) process model (Brown & Hwang, 1992). . . . We model the continuous change in the HiBall state with the simple differential equation </p>

Exhibit E-6

CLAIM 4	Welch 2001
	<div data-bbox="520 240 1283 764">$\frac{d}{dt}\bar{x}(t) = \begin{bmatrix} 0 & 1 \\ 0 & 0 \end{bmatrix} \begin{bmatrix} x_p(t) \\ x_v(t) \end{bmatrix} + \begin{bmatrix} 0 \\ \mu \end{bmatrix} u(t), \quad (1)$<p>where $u(t)$ is a normally distributed white (in the frequency spectrum) scalar noise process, and the scalar μ represents the magnitude or spectral density of the noise. We use a similar model with a distinct noise process for each of the six pose elements. We determine the individual noise magnitudes using an offline simulation of the system and a nonlinear optimization strategy that seeks to minimize the variance between the estimated pose and a known motion path. (See section 6.2.2.).</p></div> <p data-bbox="520 805 861 836">Welch 2001 at Section 5.3.</p> <p data-bbox="520 873 1965 1019">The differential equation (1) represents a continuous integrated random walk, or an integrated Wiener or Brownian-motion process. Specifically, we model each component of the linear and angular HiBall velocities as a random walk, and then use these (assuming constant intermeasurement velocity) to estimate the HiBall pose at time $t + \delta t$ as follows:</p>

Exhibit E-6

CLAIM 4	Welch 2001
	$\bar{x}(t + \delta t) = \begin{bmatrix} 1 & \delta t \\ 0 & 1 \end{bmatrix} \bar{x}(t) \quad (2)$ <p>for each of the six pose elements. In addition to a relatively simple process model, the HiBall measurement model is relatively simple. For any ceiling LED (section 4.2) and HiBall view (section 4.1), the 2-D sensor measurement can be modeled as</p> $\begin{bmatrix} u \\ v \end{bmatrix} = \begin{bmatrix} c_x/c_z \\ c_y/c_z \end{bmatrix} \quad (3)$ <p>where</p> $\begin{bmatrix} c_x \\ c_y \\ c_z \end{bmatrix} = VR^T(\bar{l}_{xyz} - \bar{x}_{xyz}), \quad (4)$ <p>V is the camera viewing matrix from section 5.1, \bar{l}_{xyz} is the position of the LED in the world, \bar{x}_{xyz} is the position of the HiBall in the world, and R is a rotation matrix corresponding to the orientation of the HiBall in the world. In practice, we maintain the orientation of the HiBall as a combination of a global (external to the state) quaternion and a set of incremental angles as described by Welch (1996) and Welch and Bishop (1997).</p> <p>Welch 2001 at Section 5.3.</p>

Exhibit E-6

CLAIM 4	Welch 2001
	<p>Because the measurement model (3) and (4) is non-linear, we use an extended Kalman filter, making use of the Jacobian of the nonlinear HiBall measurement model to transform the covariance of the Kalman filter. Welch 2001 at Section 5.3.</p> <p>Along with the benefit of simplicity and speed, the SCAAT approach offers the additional capability of being able to estimate the 3-D positions of the LEDs in the world concurrently with the pose of the HiBall, online, in real time. This capability is a tremendous benefit in terms of the accuracy and noise characteristics of the estimates.</p>

Exhibit E-6

CLAIM 4	Welch 2001
	<p data-bbox="535 248 1276 1109">The method we now use for autocalibration involves defining a distinct SCAAT Kalman filter for each LED. Specifically, for each LED, we maintain a state \bar{l} (estimate of the 3-D position) and a 3×3 Kalman filter covariance. At the beginning of each estimation cycle, we form an augmented state vector \hat{x} using the appropriate LED state and the current HiBall state: $\hat{x} = [\bar{x}^T, \bar{l}^T]^T$. Similarly, we augment the Kalman filter error covariance matrix with that of the LED filter. We then follow the normal steps outlined in section 5.3, with the result being that the LED portion of the filter state and covariance is updated in accordance with the measurement residual. At the end of the cycle, we extract the LED portions of the state and covariance from the augmented filter, and save them externally. The effect is that, as the system is being used, it continually refines its estimates of the LED positions, thereby continually improving its estimates of the HiBall pose. Again, for additional information, see Welch (1996) and Welch and Bishop (1997).</p> <p data-bbox="514 1157 861 1190">Welch 2001 at Section 5.4.</p> <p data-bbox="514 1227 1957 1369">The recursive nature of the Kalman filter (section 5.3) requires that the filter be initialized with a known state and corresponding covariance before steady-state operation can begin. Such an initialization (or acquisition) must take place prior to any tracking session, but also upon the (rare) occasion when the filter diverges and “loses lock” as a result of blocked sensor views, for example.</p> <p data-bbox="514 1373 861 1406">Welch 2001 at Section 5.5.</p>

Exhibit E-6

CLAIM 4	Welch 2001
	<p><i>See</i> Disclosures with respect to Claim 2, <i>supra</i>; <i>see also</i> Defendants' Invalidity Contentions for further discussion.</p>

E. INDEPENDENT CLAIM 6

CLAIM 6	Welch 2001
<p>[6.pre] A method comprising:</p>	<p>At least under Plaintiffs' apparent infringement theory, Welch 2001 discloses, either expressly or inherently, a method. In the alternative, this element would be obvious over Welch 2001 in light of the other references disclosed in Defendants' Invalidity Contentions and/or the knowledge of one of ordinary skill in the art.</p> <p><i>See, e.g.:</i></p> <p>We present results and a complete description of our most recent electro-optical system, the HiBall Tracking System. In particular, we discuss motivation for the geometric configuration and describe the novel optical, mechanical, electronic, and algorithmic aspects that enable unprecedented speed, resolution, accuracy, robustness, and flexibility.</p> <p>Welch 2001 at Abstract.</p> <p>Systems for head tracking for interactive computer graphics have been explored for more than thirty years. Welch 2001 at Section 1.</p> <p>As part of his 1984 dissertation on Self-Tracker, Bishop put forward the idea of outward-looking tracking systems based on user-mounted sensors that estimate user pose by observing landmarks in the environment (Bishop, 1984). He described two kinds of landmarks: high signal-to-noise-ratio beacons such as light-emitting diodes (LEDs) and low signal-to-noise-ratio landmarks such as naturally occurring features. Bishop designed and demonstrated custom VLSI chips (figure 2) that combined image sensing and processing on a single chip (Bishop & Fuchs, 1984). The idea was to combine multiple instances of these chips into an outward-looking cluster that estimated cluster motion by observing natural features in the unmodified environment. Integrating the resulting motion to estimate pose is prone to accumulating error, so further development required a</p>

Exhibit E-6

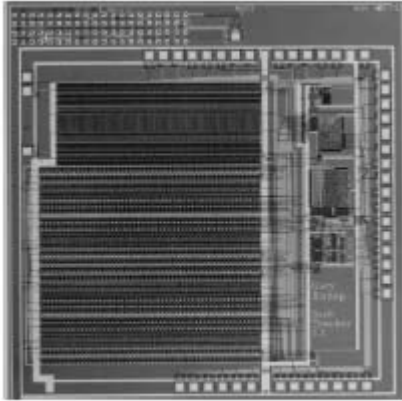
CLAIM 6	Welch 2001
	<p data-bbox="514 240 1648 308">complementary system based on easily detectable landmarks (LEDs) at known locations. Welch 2001 at Section 1.2.</p> <div data-bbox="514 344 959 828">  <p data-bbox="541 779 661 812">Figure 2.</p> </div> <p data-bbox="514 868 1942 1161">In 1991, we demonstrated a working, scalable, electro-optical head-tracking system in the Tomorrow's Realities gallery at that year's ACM SIGGRAPH conference (Wang et al., 1990; Wang, Chi, & Fuchs, 1990; Ward et al., 1992). The system (figure 3) used four, head-worn, lateral-effect photodiodes that looked upward at a regular array of infrared LEDs installed in precisely machined ceiling panels. A user-worn backpack contained electronics that digitized and communicated the photo-coordinates of the sighted LEDs. Photogrammetric techniques were used to compute a user's head pose using the known LED positions and the corresponding measured photo-coordinates from each LEPD sensor (Azuma & Ward, 1991). Welch 2001 at Section 1.2.</p>

Exhibit E-6


CLAIM 6	Welch 2001
	

Exhibit E-6

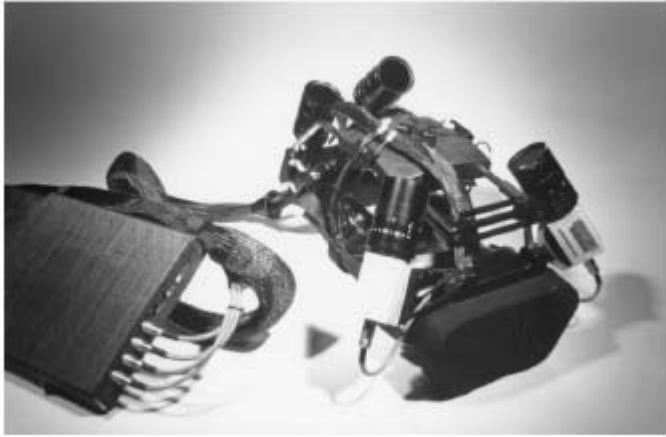
CLAIM 6	Welch 2001
	<div data-bbox="520 240 1255 755">  <p data-bbox="520 706 640 738">Figure 3.</p> </div> <p data-bbox="510 787 1365 820"><i>See also</i> Defendants' Invalidity Contentions for further discussion.</p>
<p data-bbox="153 885 468 1169">[6.a] enumerating sensing elements available to a tracking system that includes an estimation subsystem that estimates a position or orientation of an object; and</p>	<p data-bbox="510 885 1969 1055">At least under Plaintiffs' apparent infringement theory, Welch 2001 discloses, either expressly or inherently, enumerating sensing elements available to a tracking system that includes an estimation subsystem that estimates a position or orientation of an object. In the alternative, this element would be obvious over Welch 2001 in light of the other references disclosed in Defendants' Invalidity Contentions and/or the knowledge of one of ordinary skill in the art.</p> <p data-bbox="510 1096 630 1128"><i>See, e.g.:</i></p> <p data-bbox="510 1161 1921 1421">Thanks to significant improvements in hardware and software, this HiBall system offers unprecedented speed, resolution, accuracy, robustness, and flexibility. The bulky and heavy sensors and backpack of the previous system have been replaced by a small HiBall unit (figure 4, bottom). In addition, the precisely machined LED ceiling panels of the previous system have been replaced by looser-tolerance panels that are relatively inexpensive to make and simple to install (figure 4, top; figure 10). Finally, we are using an unusual Kalman-filter-based algorithm that generates very accurate pose estimates at a high rate with low latency, and that simultaneously self-calibrates the system.</p>

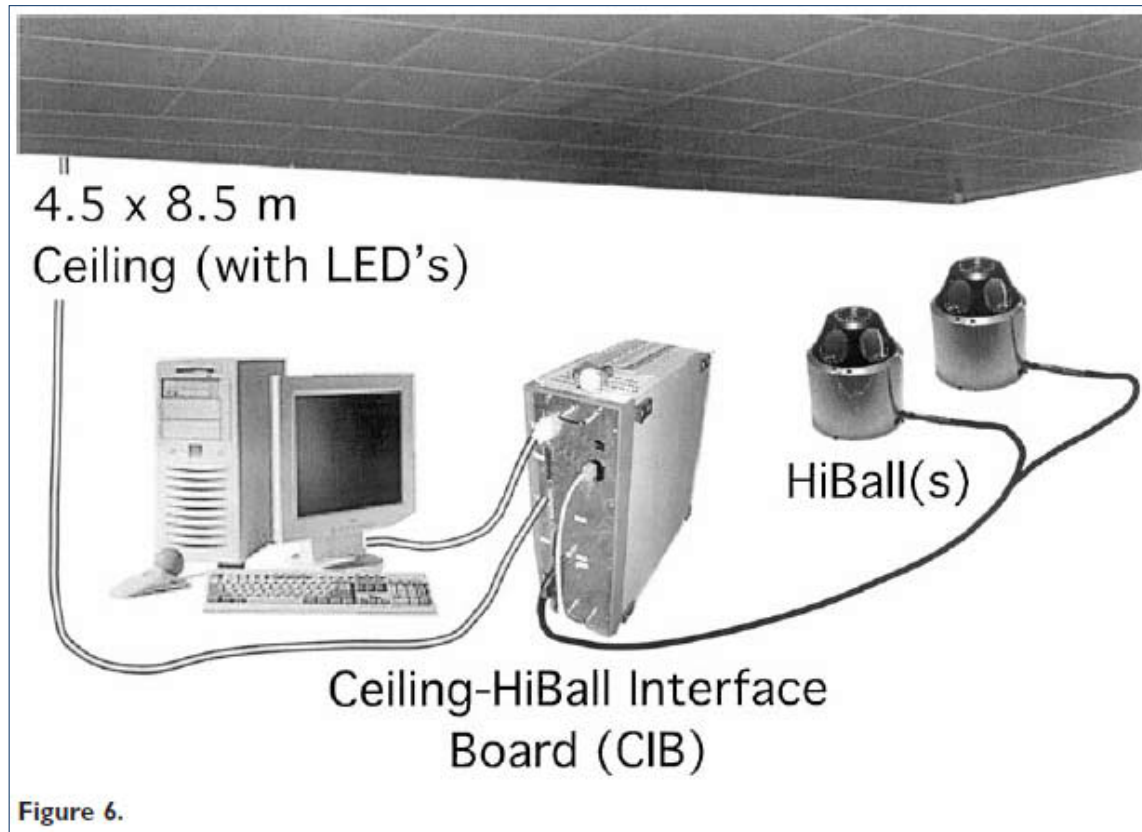
Exhibit E-6

CLAIM 6	Welch 2001
	<p>As a result of these improvements, the HiBall Tracking System can generate more than 2,000 pose estimates per second, with less than 1 ms of latency, better than 0.5 mm and 0.03 deg. of absolute error and noise, everywhere in a 4.5 m x 8.5 m room (with more than two meters of height variation). The area can be expanded by adding more panels, or by using checker-board configurations that spread panels over a larger area. The weight of the user-worn HiBall is approximately 300 grams, making it lighter than one optical sensor in the 1991 system. Multiple HiBall units can be daisy-chained together for head or hand tracking, pose-aware input devices, or precise 3-D point digitization throughout the entire working volume.</p> <p>Welch 2001 at Section 1.3.</p> <p>The HiBall Tracking System consists of three main components (figure 6). An outward-looking sensing unit we call the HiBall is fixed to each user to be tracked. The HiBall unit observes a subsystem of fixed-location infrared LEDs we call the Ceiling. Communication and synchronization between the host computer and these subsystems is coordinated by the Ceiling-HiBall Interface Board (CIB).</p> <p>Welch 2001 at Section 3.</p>

Exhibit E-6

CLAIM 6

Welch 2001



HiBall observes LEDs through multiple sensor-lens views that are distributed over a large solid angle. LEDs are sequentially flashed (one at a time) such that they are seen via a diverse set of views for each HiBall. Initial acquisition is performed using a brute-force search through LED space, but, once initial lock is made, the selection of LEDs to flash is tailored to the views of the active HiBall units. Pose estimates are maintained using a Kalman-filter-based prediction-correction approach known as single-constraint-at-a-time (SCAAT) tracking. This technique has been extended to provide self-calibration of the ceiling, concurrent with HiBall tracking.

Welch 2001 at Section 3.

Exhibit E-6

CLAIM 6	Welch 2001
	<p>The original electro-optical tracker (figure 3, bottom) used independently housed lateral-effect photodiode units (LEPDs) attached to a lightweight tubular framework. As it turns out, the mechanical framework would flex (distort) during use, contributing to estimation errors. In part to address this problem, the HiBall sensor unit was designed as a single, rigid, hollow ball having dodecahedral symmetry, with lenses in the upper six faces and LEPDs on the insides of the opposing six lower faces (figure 7). This immediately gives six primary “camera” views uniformly spaced by 57 deg. The views efficiently share the same internal air space and are rigid with respect to each other. In addition, light entering any lens sufficiently off-axis can be seen by a neighboring LEPD, giving rise to five secondary views through the top or central lens, and three secondary views through the five other lenses. Overall, this provides 26 fields of view that are used to sense widely separated groups of LEDs in the environment. Although the extra views complicate the initialization of the Kalman filter as described in section 5.5, they turn out to be of great benefit during steady-state tracking by effectively increasing the overall HiBall field of view without sacrificing optical-sensor resolution.</p> <p>Welch 2001 at Section 4.1</p> <p>HiBall sensor unit was designed as a single, rigid, hollow ball having dodecahedral symmetry, with lenses in the upper six faces and LEPDs on the insides of the opposing six lower faces (figure 7). This immediately gives six primary “camera” views uniformly spaced by 57 deg. The views efficiently share the same internal air space and are rigid with respect to each other. In addition, light entering any lens sufficiently off-axis can be seen by a neighboring LEPD, giving rise to five secondary views through the top or central lens, and three secondary views through the five other lenses. Overall, this provides 26 fields of view that are used to sense widely separated groups of LEDs in the environment.</p> <p>Welch 2001 at Section 4.1.</p>

Exhibit E-6

CLAIM 6	Welch 2001
	<div data-bbox="527 250 974 683" data-label="Image"> </div> <div data-bbox="527 716 974 1049" data-label="Image"> </div> <div data-bbox="525 1066 651 1102" data-label="Caption"> <p>Figure 7.</p> </div> <div data-bbox="504 1146 1974 1403" data-label="Text"> <p>The LEPDs themselves are not imaging devices; rather, they detect the centroid of the luminous flux incident on the detector. The x-position of the centroid determines the ratio of two output y-position determines the ratio of two other output currents. The total output current of each pair are commensurate and are proportional to the total incident flux. Consequently, focus is not an issue, so the simple fixed-focus lenses work well over a range of LED distances from about half a meter to infinity. The LEPDs and associated electronic components are mounted on a custom rigid-flex printed circuit board (figure 8). This arrangement makes efficient use of the internal HiBall volume while maintaining isolation between analog and</p> </div>

Exhibit E-6

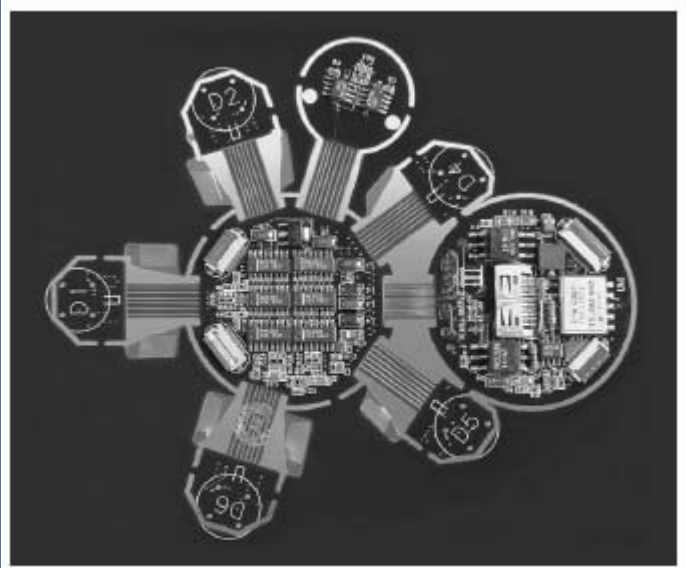
CLAIM 6	Welch 2001
	<p>digital circuitry, and increasing reliability by alleviating the need for intercomponent mechanical connectors. Welch 2001 at Section 4.1.</p> <div data-bbox="520 347 1201 911">  </div> <p>Figure 8.</p> <p>Figure 9 shows the physical arrangement of the folded electronics in the HiBall. Each LEPD has four transimpedance amplifiers (shown together as one “Amp” in figure 9), the analog outputs of which are multiplexed with those of the other LEPDs, then sampled, held, and converted by four 16-bit Delta-Sigma analog-to-digital (A/D) converters. Multiple samples are integrated via an accumulator. The digitized LEPD data are organized into packets for communication back to the CIB. The packets also contain information to assist in error detection. The communication protocol is simple, and, while presently implemented by wire, the modulation scheme is amenable to a wireless implementation. Welch 2001 at Section 4.1.</p> <p>The Ceiling-HiBall Interface Board (CIB) (figure 11) provides communication and synchronization between a host personal computer, the HiBall (section 4.1), and the ceiling (section 4.2). The CIB has four ceiling ports allowing interleaving of ceiling panels for up to four simultaneous LED flashes and/or higher ceiling bandwidth.</p>

Exhibit E-6

CLAIM 6	Welch 2001
	<p>(The ceiling bandwidth is inherently limited by LED power restrictions as described in section 4.2, but this can be increased by spatially multiplexing the ceiling panels.) The CIB has two tether interfaces that can communicate with up to four daisy-chained HiBall units. The full-duplex communication with the HiBall units uses a modulation scheme (BPSK) allowing future wireless operation. The interface from the CIB to the host PC is the stable IEEE1284C extended parallel port (EPP) standard.</p> <p>The CIB comprises analog drive and receive components as well as digital logic components. The digital components implement store and forward in both directions and synchronize the timing of the LED “on” interval within the HiBall dark-light-dark intervals (section 5.2). The protocol supports full-duplex flow control. The data are arranged into packets that incorporate error detection.</p> <p>Welch 2001 at Section 4.3.</p>

Exhibit E-6

CLAIM 6	Welch 2001
	<div data-bbox="520 240 1528 1003"> <p>Figure 9.</p> </div> <p>This multiple constraint method had several drawbacks. First, it had a significantly lower estimate rate due to the need to collect multiple measurements per estimate. Second, the system of nonlinear equations did not account for the fact that the sensor fixture continued to move throughout the collection of the sequence of measurements. Instead, the method effectively assumes that the measurements were taken simultaneously. The violation of this simultaneity assumption could introduce significant error during even moderate motion. Finally, the method provided no means to identify or handle unusually noisy individual measurements. Thus, a single erroneous measurement could cause an estimate to jump away from an otherwise smooth track.</p> <p>Welch 2001 at Section 5.3.</p>

Exhibit E-6

CLAIM 6	Welch 2001
	<p>Once a particular view and LED have been chosen in this fashion, the CIB (section 4.3) is instructed to flash the LED and take a measurement as described in section 5.2. This single measurement is compared with a prediction obtained using equation (3), and the difference (or residual) is used to update the filter state and covariance matrices using the Kalman gain matrix. The Kalman gain is computed as a combination of the current filter covariance, the measurement noise variance (section 6.2.1), and the Jacobian of the measurement model. This recursive prediction-correction cycle continues in an ongoing fashion, a single constraint at a time.</p> <p>Welch 2001 at Section 5.3.</p> <p>The online measurements (section 5.2) are used to estimate the pose of the HiBall during operation. The 1991 system collected a group of diverse measurements for a variety of LEDs and sensors, and then used a method of simultaneous nonlinear equations called collinearity (Azuma & Ward, 1991) to estimate the pose of the sensor fixture shown in figure 3 (bottom).</p> <p>Welch 2001 at Section 5.3.</p> <p>In contrast, the approach we use with the new HiBall system produces tracker reports as each new measurement is made, rather than waiting to form a complete collection of observations. Because single measurements under constrain the mathematical solution, we refer to the approach as single-constraint-at-a-time (SCAAT) tracking (Welch, 1996; Welch & Bishop, 1997). The key is that the single measurements provide some information about the HiBall's state, and thus can be used to incrementally improve a previous estimate. We intentionally fuse each individual "insufficient" measurement immediately as it is obtained. With this approach, we are able to generate estimates more frequently, with less latency, and with improved accuracy, and we are able to estimate the LED positions online concurrently while tracking the HiBall (section 5.4).</p> <p>Welch 2001 at Section 5.3.</p> <p>We use a Kalman filter (Kalman, 1960) to fuse the measurements into an estimate of the HiBall state x (the pose of the HiBall). We use the Kalman filter—a minimum-variance stochastic estimator—both because the sensor measurement noise and the typical user-motion dynamics can be modeled as normally distributed random processes, and because we want an efficient online method of estimation.</p> <p>Welch 2001 at Section 5.3.</p> <p>The Kalman filter has been used previously to address similar or related problems. . . . A relevant example of a Kalman filter used for sensor fusion in a wide-area tracking system is given in Foxlin et al. (1998), which</p>

Exhibit E-6


CLAIM 6	Welch 2001
	<p data-bbox="514 240 1770 308">describes a hybrid inertial-acoustic system that is commercially available today (Intersense, 2000). Welch 2001 at Section 5.3.</p> <p data-bbox="514 345 1955 558">[O]ne key benefit warrants discussion here. There is a direct relationship between the complexity of the estimation algorithm, the corresponding speed (execution time per estimation cycle), and the change in HiBall pose between estimation cycles (figure 12). As the algorithmic complexity increases, the execution time increases, which allows for significant nonlinear HiBall motion between estimation cycles, which in turn implies the need for a more complex estimation algorithm. Welch 2001 at Section 5.3.</p> <div data-bbox="520 597 1142 1289"><p data-bbox="533 1256 663 1284">Figure 12.</p></div> <p data-bbox="514 1328 1927 1435">The SCAAT approach, on the other hand, is an attempt to reverse this cycle. Because we intentionally use a single constraint per estimate, the algorithmic complexity is drastically reduced, which reduces the execution time, and hence the amount of motion between estimation cycles. Because the amount of motion is limited, we</p>

Exhibit E-6

CLAIM 6	Welch 2001
	<p>are able to use a simple dynamic (process) model in the Kalman filter, which further simplifies the computations. In short, the simplicity of the approach means that it can run very fast, which means it can produce estimates very rapidly, with low noise.</p> <p>Welch 2001 at Section 5.3.</p> <p>The Kalman filter requires both a model of the process dynamics and a model of the relationship between the process state and the available measurements. In part due to the simplicity of the SCAAT approach, we are able to use a simple position-velocity (PV) process model (Brown & Hwang, 1992). . . . We model the continuous change in the HiBall state with the simple differential equation</p> <div data-bbox="520 597 1283 1122" style="border: 1px solid black; padding: 10px; margin: 10px 0;"> $\frac{d}{dt}\bar{x}(t) = \begin{bmatrix} 0 & 1 \\ 0 & 0 \end{bmatrix} \begin{bmatrix} x_p(t) \\ x_v(t) \end{bmatrix} + \begin{bmatrix} 0 \\ \mu \end{bmatrix} u(t), \quad (1)$ <p>where $u(t)$ is a normally distributed white (in the frequency spectrum) scalar noise process, and the scalar μ represents the magnitude or spectral density of the noise. We use a similar model with a distinct noise process for each of the six pose elements. We determine the individual noise magnitudes using an offline simulation of the system and a nonlinear optimization strategy that seeks to minimize the variance between the estimated pose and a known motion path. (See section 6.2.2.).</p> </div> <p>Welch 2001 at Section 5.3.</p> <p>The differential equation (1) represents a continuous integrated random walk, or an integrated Wiener or Brownian-motion process. Specifically, we model each component of the linear and angular HiBall velocities as a random walk, and then use these (assuming constant intermeasurement velocity) to estimate the HiBall pose at time $t + \delta t$ as follows:</p>

Exhibit E-6

CLAIM 6	Welch 2001
	$\bar{x}(t + \delta t) = \begin{bmatrix} 1 & \delta t \\ 0 & 1 \end{bmatrix} \bar{x}(t) \quad (2)$ <p>for each of the six pose elements. In addition to a relatively simple process model, the HiBall measurement model is relatively simple. For any ceiling LED (section 4.2) and HiBall view (section 4.1), the 2-D sensor measurement can be modeled as</p> $\begin{bmatrix} u \\ v \end{bmatrix} = \begin{bmatrix} c_x/c_z \\ c_y/c_z \end{bmatrix} \quad (3)$ <p>where</p> $\begin{bmatrix} c_x \\ c_y \\ c_z \end{bmatrix} = VR^T(\bar{l}_{xyz} - \bar{x}_{xyz}), \quad (4)$ <p>V is the camera viewing matrix from section 5.1, \bar{l}_{xyz} is the position of the LED in the world, \bar{x}_{xyz} is the position of the HiBall in the world, and R is a rotation matrix corresponding to the orientation of the HiBall in the world. In practice, we maintain the orientation of the HiBall as a combination of a global (external to the state) quaternion and a set of incremental angles as described by Welch (1996) and Welch and Bishop (1997).</p> <p>Welch 2001 at Section 5.3.</p>

Exhibit E-6

CLAIM 6	Welch 2001
	<p>Because the measurement model (3) and (4) is non-linear, we use an extended Kalman filter, making use of the Jacobian of the nonlinear HiBall measurement model to transform the covariance of the Kalman filter. Welch 2001 at Section 5.3.</p> <p>Along with the benefit of simplicity and speed, the SCAAT approach offers the additional capability of being able to estimate the 3-D positions of the LEDs in the world concurrently with the pose of the HiBall, online, in real time. This capability is a tremendous benefit in terms of the accuracy and noise characteristics of the estimates.</p>

Exhibit E-6

CLAIM 6	Welch 2001
	<p data-bbox="535 248 1276 1109">The method we now use for autocalibration involves defining a distinct SCAAT Kalman filter for each LED. Specifically, for each LED, we maintain a state \bar{l} (estimate of the 3-D position) and a 3×3 Kalman filter covariance. At the beginning of each estimation cycle, we form an augmented state vector \hat{x} using the appropriate LED state and the current HiBall state: $\hat{x} = [\bar{x}^T, \bar{l}^T]^T$. Similarly, we augment the Kalman filter error covariance matrix with that of the LED filter. We then follow the normal steps outlined in section 5.3, with the result being that the LED portion of the filter state and covariance is updated in accordance with the measurement residual. At the end of the cycle, we extract the LED portions of the state and covariance from the augmented filter, and save them externally. The effect is that, as the system is being used, it continually refines its estimates of the LED positions, thereby continually improving its estimates of the HiBall pose. Again, for additional information, see Welch (1996) and Welch and Bishop (1997).</p> <p data-bbox="514 1157 861 1190">Welch 2001 at Section 5.4.</p> <p data-bbox="514 1227 1957 1369">The recursive nature of the Kalman filter (section 5.3) requires that the filter be initialized with a known state and corresponding covariance before steady-state operation can begin. Such an initialization (or acquisition) must take place prior to any tracking session, but also upon the (rare) occasion when the filter diverges and “loses lock” as a result of blocked sensor views, for example.</p> <p data-bbox="514 1373 861 1406">Welch 2001 at Section 5.5.</p>

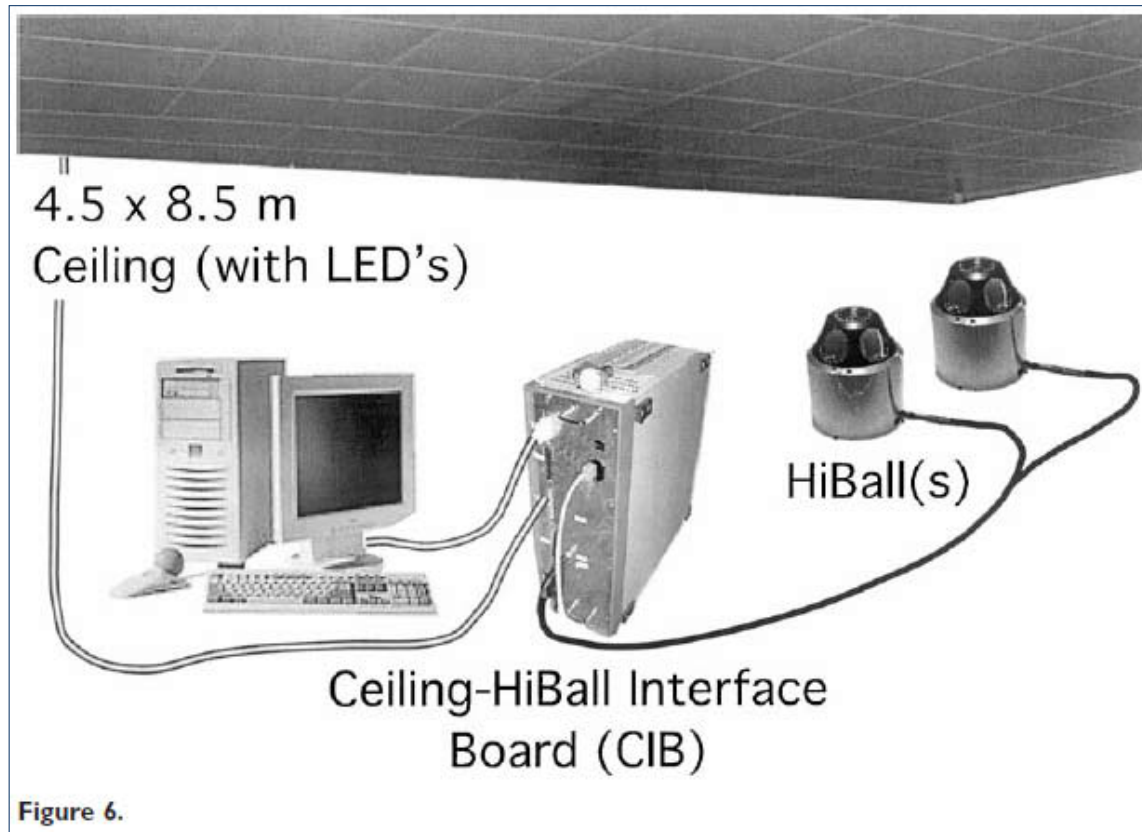
Exhibit E-6

CLAIM 6	Welch 2001
	<p>During the design of the HiBall system, we made substantial use of simulation, in some domains to a very detailed level. For example, Zemax (Focus Software, 1995) was used extensively in the design and optimization of the optical design, including the design of the filter glass lenses, and geometry of the optical-component layout.</p> <p>Welch 2001 at Section 6.2.</p> <p><i>See Defendants' Invalidity Contentions for further discussion.</i></p>
<p>[6.b] providing parameters specific to the enumerated sensing elements to the tracking system to enable the estimation subsystem to be configured based on the parameters specific to the enumerated sensing elements to enable the estimation subsystem to estimate the position or orientation of the object.</p>	<p>At least under Plaintiffs' apparent infringement theory, Welch 2001 discloses, either expressly or inherently, providing parameters specific to the enumerated sensing elements to the tracking system to enable the estimation subsystem to be configured based on the parameters specific to the enumerated sensing elements to enable the estimation subsystem to estimate the position or orientation of the object. In the alternative, this element would be obvious over Welch 2001 in light of the other references disclosed in Defendants' Invalidity Contentions and/or the knowledge of one of ordinary skill in the art.</p> <p><i>See, e.g.:</i></p> <p>Thanks to significant improvements in hardware and software, this HiBall system offers unprecedented speed, resolution, accuracy, robustness, and flexibility. The bulky and heavy sensors and backpack of the previous system have been replaced by a small HiBall unit (figure 4, bottom). In addition, the precisely machined LED ceiling panels of the previous system have been replaced by looser-tolerance panels that are relatively inexpensive to make and simple to install (figure 4, top; figure 10). Finally, we are using an unusual Kalman-filter-based algorithm that generates very accurate pose estimates at a high rate with low latency, and that simultaneously self-calibrates the system.</p> <p>Welch 2001 at Section 1.3.</p> <p>The HiBall Tracking System consists of three main components (figure 6). An outward-looking sensing unit we call the HiBall is fixed to each user to be tracked. The HiBall unit observes a subsystem of fixed-location infrared LEDs we call the Ceiling. Communication and synchronization between the host computer and these subsystems is coordinated by the Ceiling-HiBall Interface Board (CIB).</p> <p>Welch 2001 at Section 3.</p>

Exhibit E-6

CLAIM 6

Welch 2001



HiBall observes LEDs through multiple sensor-lens views that are distributed over a large solid angle. LEDs are sequentially flashed (one at a time) such that they are seen via a diverse set of views for each HiBall. Initial acquisition is performed using a brute-force search through LED space, but, once initial lock is made, the selection of LEDs to flash is tailored to the views of the active HiBall units. Pose estimates are maintained using a Kalman-filter-based prediction-correction approach known as single-constraint-at-a-time (SCAAT) tracking. This technique has been extended to provide self-calibration of the ceiling, concurrent with HiBall tracking.

Welch 2001 at Section 3.

Exhibit E-6

CLAIM 6	Welch 2001
	<p>The original electro-optical tracker (figure 3, bottom) used independently housed lateral-effect photodiode units (LEPDs) attached to a lightweight tubular framework. As it turns out, the mechanical framework would flex (distort) during use, contributing to estimation errors. In part to address this problem, the HiBall sensor unit was designed as a single, rigid, hollow ball having dodecahedral symmetry, with lenses in the upper six faces and LEPDs on the insides of the opposing six lower faces (figure 7). This immediately gives six primary “camera” views uniformly spaced by 57 deg. The views efficiently share the same internal air space and are rigid with respect to each other. In addition, light entering any lens sufficiently off-axis can be seen by a neighboring LEPD, giving rise to five secondary views through the top or central lens, and three secondary views through the five other lenses. Overall, this provides 26 fields of view that are used to sense widely separated groups of LEDs in the environment. Although the extra views complicate the initialization of the Kalman filter as described in section 5.5, they turn out to be of great benefit during steady-state tracking by effectively increasing the overall HiBall field of view without sacrificing optical-sensor resolution.</p> <p>Welch 2001 at Section 4.1</p> <p>HiBall sensor unit was designed as a single, rigid, hollow ball having dodecahedral symmetry, with lenses in the upper six faces and LEPDs on the insides of the opposing six lower faces (figure 7). This immediately gives six primary “camera” views uniformly spaced by 57 deg. The views efficiently share the same internal air space and are rigid with respect to each other. In addition, light entering any lens sufficiently off-axis can be seen by a neighboring LEPD, giving rise to five secondary views through the top or central lens, and three secondary views through the five other lenses. Overall, this provides 26 fields of view that are used to sense widely separated groups of LEDs in the environment.</p> <p>Welch 2001 at Section 4.1.</p>

Exhibit E-6

CLAIM 6	Welch 2001
	<div data-bbox="527 250 974 683" data-label="Image"> </div> <div data-bbox="527 719 974 1052" data-label="Image"> </div> <div data-bbox="525 1066 651 1102" data-label="Caption"> <p>Figure 7.</p> </div> <div data-bbox="504 1146 1982 1403" data-label="Text"> <p>The LEPDs themselves are not imaging devices; rather, they detect the centroid of the luminous flux incident on the detector. The x-position of the centroid determines the ratio of two output y-position determines the ratio of two other output currents. The total output current of each pair are commensurate and are proportional to the total incident flux. Consequently, focus is not an issue, so the simple fixed-focus lenses work well over a range of LED distances from about half a meter to infinity. The LEPDs and associated electronic components are mounted on a custom rigid-flex printed circuit board (figure 8). This arrangement makes efficient use of the internal HiBall volume while maintaining isolation between analog and</p> </div>

Exhibit E-6

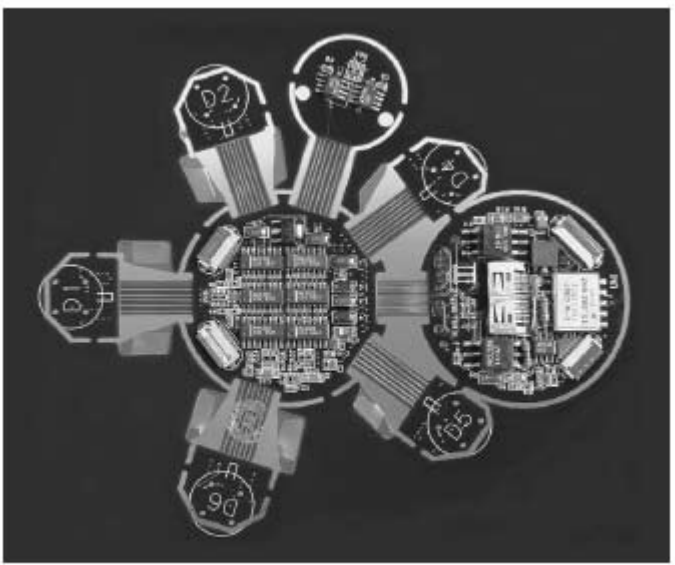
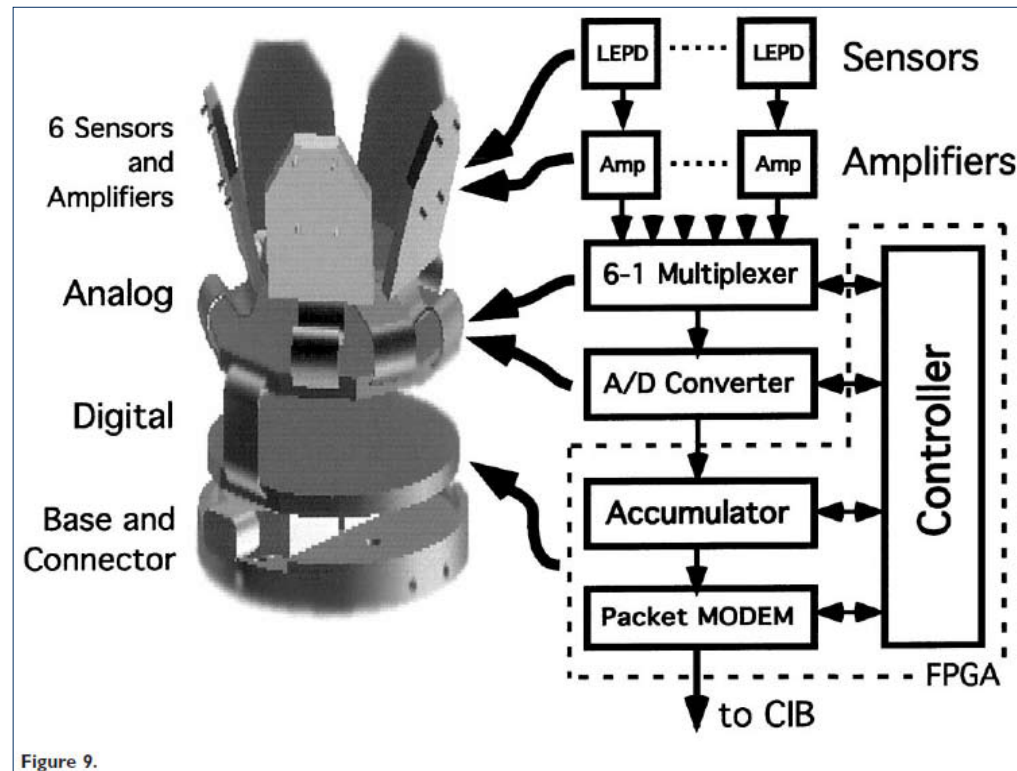
CLAIM 6	Welch 2001
	<p>digital circuitry, and increasing reliability by alleviating the need for intercomponent mechanical connectors. Welch 2001 at Section 4.1.</p> <div data-bbox="520 345 1203 971">  <p>Figure 8.</p> </div> <p>Figure 9 shows the physical arrangement of the folded electronics in the HiBall. Each LEPD has four transimpedance amplifiers (shown together as one “Amp” in figure 9), the analog outputs of which are multiplexed with those of the other LEPDs, then sampled, held, and converted by four 16-bit Delta-Sigma analog-to-digital (A/D) converters. Multiple samples are integrated via an accumulator. The digitized LEPD data are organized into packets for communication back to the CIB. The packets also contain information to assist in error detection. The communication protocol is simple, and, while presently implemented by wire, the modulation scheme is amenable to a wireless implementation. Welch 2001 at Section 4.1.</p> <p>The CIB comprises analog drive and receive components as well as digital logic components. The digital components implement store and forward in both directions and synchronize the timing of the LED “on” interval within the HiBall dark-light-dark intervals (section 5.2). The protocol supports full-duplex flow control. The data</p>

Exhibit E-6

CLAIM 6

Welch 2001

are arranged into packets that incorporate error detection.
Welch 2001 at Section 4.3.



After each HiBall is assembled, we perform an offline calibration procedure to determine the correspondence between image-plane coordinates and rays in space. This involves more than just determining the view transform for each of the 26 views. Nonlinearities in the silicon sensor and distortions in the lens (such as spherical aberration) cause significant deviations from a simple pinhole camera model. We dealt with all of these issues through the use of a two-part camera model. The first part is a standard pinhole camera represented by a 3 X 4 matrix. The second part is a table mapping real

Exhibit E-6

CLAIM 6	Welch 2001
	<p>image-plane coordinates to ideal image-plane coordinates. Welch 2001 at Section 5.1.</p> <p>Both parts of the camera model are determined using a calibration procedure that relies on a goniometer (an angular positioning system) of our own design. This device consists of two servo motors mounted together such that one motor provides rotation about the vertical axis while the second motor provides rotation about an axis orthogonal to vertical. An important characteristic of the goniometer is that the rotational axes of the two motors intersect at a point at the center of the HiBall optical sphere; this point is defined as the origin of the HiBall. . . . The rotational positioning motors were rated to provide twenty arc-second precision; we further calibrated them to six arc seconds using a laboratory grade theodolite—an angle measuring system. Welch 2001 at Section 5.1.</p> <p>To determine the mapping between sensor image-plane coordinates and three-space rays, we use a single LED mounted at a fixed location in the laboratory such that it is centered in the view directly out of the top lens of the HiBall. This ray defines the z or up axis for the HiBall coordinate system. We sample other rays by rotating the goniometer motors under computer control. We sample each view with rays spaced about every six minutes of arc throughout the field of view. We repeat each measurement 100 times to reduce the effects of noise on the individual measurements and to estimate the standard deviation of the measurements. Welch 2001 at Section 5.1.</p> <p>Given the tables of approximately 2,500 measurements for each of the 26 views, we first determine a 3 X 4 view matrix using standard linear least-squares techniques. Then, we determine the deviation of each measured point from that predicted by the ideal linear model. These deviations are resampled into a 25 X 25 grid indexed by sensor-plane coordinates using a simple scan-conversion procedure and averaging. Given a measurement from a sensor at runtime (section 5.2), we convert it to an “ideal” measurement by subtracting a deviation bilinearly interpolated from the nearest four entries in the table. Welch 2001 at Section 5.1.</p> <p>Upon receiving a command from the CIB (section 4.3), which is synchronized with a CIB command to the ceiling, the HiBall selects the specified LEPD and performs three measurements, one before the LED flashes, one during the LED flash, and one after the LED flash. Known as “dark-light-dark,” this technique is used to subtract out DC bias, low-frequency noise, and background light from the LED signal.</p>

Exhibit E-6

CLAIM 6	Welch 2001
	<p data-bbox="514 240 1871 310">We then convert the measured sensor coordinates to “ideal” coordinates using the calibration tables described in section 5.1.</p> <p data-bbox="514 345 1948 670">In addition, during runtime we attempt to maximize the signal-to-noise ratio of the measurement with an automatic gain-control scheme. For each LED, we store a target signal strength factor. We compute the LED current and number of integrations (of successive accumulated A/D samples) by dividing this strength factor by the square of the distance to the LED, estimated from the current position estimate. After a reading, we look at the strength of the actual measurement. If it is larger than expected, we reduce the gain; if it is less than expected, we increase the gain. The increase and decrease are implemented as online averages with scaling such that the gain factor decreases rapidly (to avoid overflow) and increases slowly. Finally, we use the measured signal strength to estimate the noise on the signal using (Chi, 1995), and then use this as the measurement noise estimate for the Kalman filter (section 5.3).</p> <p data-bbox="514 706 861 735">Welch 2001 at Section 5.2.</p> <p data-bbox="514 771 1948 919">The Kalman filter requires both a model of the process dynamics and a model of the relationship between the process state and the available measurements. In part due to the simplicity of the SCAAT approach, we are able to use a simple position-velocity (PV) process model (Brown & Hwang, 1992). . . . We model the continuous change in the HiBall state with the simple differential equation</p>

Exhibit E-6

CLAIM 6	Welch 2001
	<div data-bbox="667 261 1276 337" data-label="Equation-Block"> $\frac{d}{dt}\bar{x}(t) = \begin{bmatrix} 0 & 1 \\ 0 & 0 \end{bmatrix} \begin{bmatrix} x_p(t) \\ x_v(t) \end{bmatrix} + \begin{bmatrix} 0 \\ \mu \end{bmatrix} u(t), \quad (1)$ </div> <p data-bbox="531 375 1270 753">where $u(t)$ is a normally distributed white (in the frequency spectrum) scalar noise process, and the scalar μ represents the magnitude or spectral density of the noise. We use a similar model with a distinct noise process for each of the six pose elements. We determine the individual noise magnitudes using an offline simulation of the system and a nonlinear optimization strategy that seeks to minimize the variance between the estimated pose and a known motion path. (See section 6.2.2.).</p> <p data-bbox="514 805 858 834">Welch 2001 at Section 5.3.</p> <p data-bbox="514 873 1963 1019">The differential equation (1) represents a continuous integrated random walk, or an integrated Wiener or Brownian-motion process. Specifically, we model each component of the linear and angular HiBall velocities as a random walk, and then use these (assuming constant intermeasurement velocity) to estimate the HiBall pose at time $t + \delta t$ as follows:</p>

Exhibit E-6

CLAIM 6	Welch 2001
	<div data-bbox="743 269 1272 341" data-label="Equation-Block"> $\bar{x}(t + \delta t) = \begin{bmatrix} 1 & \delta t \\ 0 & 1 \end{bmatrix} \bar{x}(t) \quad (2)$ </div> <div data-bbox="533 380 1264 581" data-label="Text"> <p>for each of the six pose elements. In addition to a relatively simple process model, the HiBall measurement model is relatively simple. For any ceiling LED (section 4.2) and HiBall view (section 4.1), the 2-D sensor measurement can be modeled as</p> </div> <div data-bbox="802 626 1272 698" data-label="Equation-Block"> $\begin{bmatrix} u \\ v \end{bmatrix} = \begin{bmatrix} c_x/c_z \\ c_y/c_z \end{bmatrix} \quad (3)$ </div> <div data-bbox="533 737 617 769" data-label="Text"> <p>where</p> </div> <div data-bbox="743 815 1272 919" data-label="Equation-Block"> $\begin{bmatrix} c_x \\ c_y \\ c_z \end{bmatrix} = VR^T(\bar{l}_{xyz} - \bar{x}_{xyz}), \quad (4)$ </div> <div data-bbox="533 958 1264 1295" data-label="Text"> <p>V is the camera viewing matrix from section 5.1, \bar{l}_{xyz} is the position of the LED in the world, \bar{x}_{xyz} is the position of the HiBall in the world, and R is a rotation matrix corresponding to the orientation of the HiBall in the world. In practice, we maintain the orientation of the HiBall as a combination of a global (external to the state) quaternion and a set of incremental angles as described by Welch (1996) and Welch and Bishop (1997).</p> </div> <div data-bbox="512 1341 861 1377" data-label="Text"> <p>Welch 2001 at Section 5.3.</p> </div>

Exhibit E-6

CLAIM 6	Welch 2001
	<p>Because the measurement model (3) and (4) is non-linear, we use an extended Kalman filter, making use of the Jacobian of the nonlinear HiBall measurement model to transform the covariance of the Kalman filter. Welch 2001 at Section 5.3.</p> <p>Along with the benefit of simplicity and speed, the SCAAT approach offers the additional capability of being able to estimate the 3-D positions of the LEDs in the world concurrently with the pose of the HiBall, online, in real time. This capability is a tremendous benefit in terms of the accuracy and noise characteristics of the estimates.</p>

Exhibit E-6

CLAIM 6	Welch 2001
	<p data-bbox="535 248 1276 1109">The method we now use for autocalibration involves defining a distinct SCAAT Kalman filter for each LED. Specifically, for each LED, we maintain a state \bar{l} (estimate of the 3-D position) and a 3×3 Kalman filter covariance. At the beginning of each estimation cycle, we form an augmented state vector \hat{x} using the appropriate LED state and the current HiBall state: $\hat{x} = [\bar{x}^T, \bar{l}^T]^T$. Similarly, we augment the Kalman filter error covariance matrix with that of the LED filter. We then follow the normal steps outlined in section 5.3, with the result being that the LED portion of the filter state and covariance is updated in accordance with the measurement residual. At the end of the cycle, we extract the LED portions of the state and covariance from the augmented filter, and save them externally. The effect is that, as the system is being used, it continually refines its estimates of the LED positions, thereby continually improving its estimates of the HiBall pose. Again, for additional information, see Welch (1996) and Welch and Bishop (1997).</p> <p data-bbox="514 1157 861 1190">Welch 2001 at Section 5.4.</p> <p data-bbox="514 1227 1957 1369">The recursive nature of the Kalman filter (section 5.3) requires that the filter be initialized with a known state and corresponding covariance before steady-state operation can begin. Such an initialization (or acquisition) must take place prior to any tracking session, but also upon the (rare) occasion when the filter diverges and “loses lock” as a result of blocked sensor views, for example.</p> <p data-bbox="514 1373 861 1406">Welch 2001 at Section 5.5.</p>

Exhibit E-6


CLAIM 6	Welch 2001
	<p data-bbox="514 240 1936 418">The acquisition process is complicated by the fact that each LEPD sees a number of different widely separated views (section 4.1). Therefore, detecting an LED provides at best an ambiguous set of potential LED directions in HiBall coordinates. Moreover, before acquisition, no assumptions can be made to limit the search space of visible LEDs. As such, a relatively slow brute-force algorithm is used to acquire lock. Welch 2001 at Section 5.5.</p> <p data-bbox="514 456 1963 852">As a result of a mechanical design tradeoff, each sensor field of view is less than six degrees. The focal length is set by the size of the sensor housing, which is set by the diameter of the sensors themselves. Energetics is also a factor, limiting how small the lenses can be while maintaining sufficient light-collecting area. As a result of these design tradeoffs, even a momentary small error in the HiBall pose estimate can cause the recursive estimates to diverge and the system to lose lock after only a few LED sightings. And yet the system is quite robust. In practice, users can jump around, crawl on the floor, lean over, even wave their hands in front of the sensors, and the system does not lose lock. During one session, we were using the HiBall as a 3-D digitization probe, a Hi-Ball on the end of a pencil-shaped fiberglass wand (figure 14, left). We laid the probe down on a table at one point, and were amazed to later notice that it was still tracking, even though it was observing only three or four LEDs near the edge of the ceiling. We picked up the probe and continued using it, without it ever losing lock.</p> <div data-bbox="514 889 1144 1185">  <p data-bbox="529 1144 661 1177">Figure 13.</p> </div>

Exhibit E-6

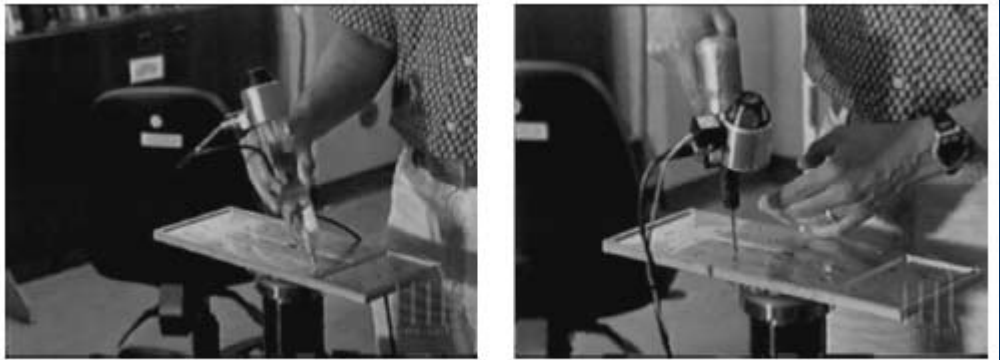
CLAIM 6	Welch 2001
	<div data-bbox="527 248 1520 605">  </div> <p data-bbox="527 626 663 656">Figure 14.</p> <p data-bbox="512 719 861 748">Welch 2001 at Section 6.1.</p> <p data-bbox="512 787 1961 1037">To make measurements of the noise when the HiBall is in motion, we rely on the assumption that almost all of the signal resulting from normal human motion is at frequencies below 2 Hz. We use a high-pass filter (Welch, 1967) on the pose estimates, and assume the output is noise. The resulting statistics are comparable to those made with the HiBall stationary, except at poses for which there are very few LEDs visible in only one or two views. In these poses, near the edge of the ceiling, the geometry of the constraints results in amplification of errors. For nearly all of the working volume of the tracker, the standard deviation of the noise on measurements while the HiBall is still or moving is about 0.2 mm and 0.03 deg.</p> <p data-bbox="512 1044 861 1073">Welch 2001 at Section 6.1.</p> <p data-bbox="512 1112 1944 1252">During the design of the HiBall system, we made substantial use of simulation, in some domains to a very detailed level. For example, Zemax (Focus Software, 1995) was used extensively in the design and optimization of the optical design, including the design of the filter glass lenses, and geometry of the optical-component layout.</p> <p data-bbox="512 1258 861 1287">Welch 2001 at Section 6.2.</p> <p data-bbox="512 1326 1961 1466">To produce realistic data for developing and tuning our algorithms, we collected several motion paths (sequences of pose estimates) from our first-generation electro-optical tracker (figure 3) at its 70 Hz maximum report rate. These paths were recorded from both naive users visiting our monthly “demo days” and from experienced users in our labs. . . . we filtered the raw path data with a noncausal zero-phase-shift, low-pass filter to eliminate energy</p>

Exhibit E-6

CLAIM 6	Welch 2001
	<p>above 2 Hz. The output of the low-pass filtering was then resampled at whatever rate we wanted to run the simulated tracker, usually 1,000 Hz. Welch 2001 at Section 6.2.</p> <p>The simulator reads camera models describing the 26 views, the sensor noise parameters, the LED positions and their expected error, and the motion path described above. Before beginning the simulation, the LED positions are perturbed from their ideal positions by adding normally distributed error to each axis. Then, for each simulated cycle of operation, the “true” poses are up- dated using the input motion path. Next, a view is chosen and a visible LED within that view is selected, and the image-plane coordinates of the LED on the chosen sensor are computed using the camera model for the view and the LED as described in section 5.3. These sensor coordinates are then perturbed based on the sensor noise model (section 6.2.1) using the distance and angle to the LED. These noise-corrupted sensor readings are then fed to the SCAAT filter to produce an updated position estimate. The position estimate is compared to the true position to produce a scalar error metric that is described next. Welch 2001 at Section 6.2.</p> <p>The error metric we used combines the error in pose in a way that relates to the effects of tracker error on a head-worn display user. We define a set of points arrayed around the user in a fixed configuration. We compute two sets of coordinates for these points: the true position using the true pose and their estimated position using the estimated pose. The error metric is then the sum of the distances between the true and estimated positions of these points. By adjusting the distance of the points from the user, we can control the relative importance of the orientation and the position error in the combined error metric. If the distance is small, then the position error is weighted most heavily; if the distance is large, then the orientation error is weighted most heavily. Our two error metrics for the entire run are the square root of the sum of the squares of all the distances, and the peak distance. Welch 2001 at Section 6.2.</p> <p><i>See also</i> Defendants’ Invalidity Contentions for further discussion.</p>

Exhibit E-6

F. DEPENDENT CLAIM 8

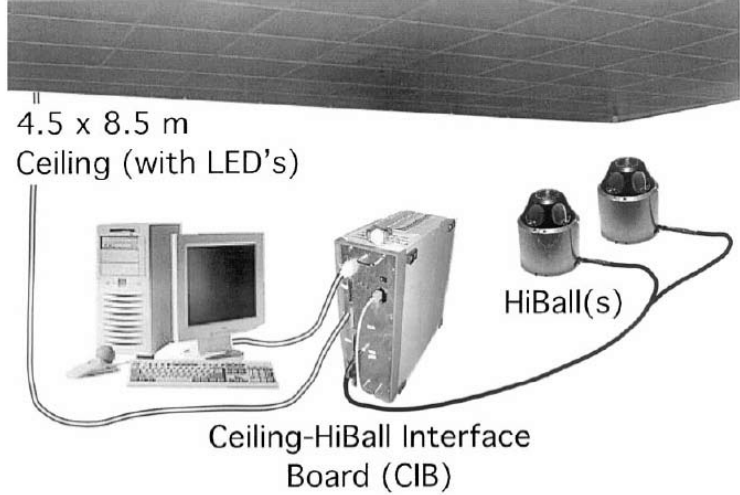
CLAIM 8	Welch 2001
<p>[8] The method of claim 6 wherein the set of sensing elements comprises at least one sensor and at least one target, the sensor making a measurement with respect to the target.</p>	<p>At least under Plaintiffs' apparent infringement theory, Welch 2001 discloses, either expressly or inherently, the method of claim 6 wherein the set of sensing elements comprises at least one sensor and at least one target, the sensor making a measurement with respect to the target. In the alternative, this element would be obvious over Welch 2001 in light of the other references disclosed in Defendants' Invalidity Contentions and/or the knowledge of one of ordinary skill in the art.</p> <p><i>See, e.g.:</i></p>  <p>Figure 6.</p> <p>Welch 2001 at Fig. 6.</p> <p>HiBall observes LEDs through multiple sensor-lens views that are distributed over a large solid angle. LEDs are sequentially flashed (one at a time) such that they are seen via a diverse set of views for each HiBall. Initial acquisition is performed using a brute-force search through LED space, but, once initial lock is made, the selection of LEDs to flash is tailored to the views of the active HiBall units. Pose estimates are maintained using a Kalman-filter-based prediction-correction approach known as single-constraint-at-</p>



Exhibit E-6

CLAIM 8	Welch 2001
	<p>a-time (SCAAT) tracking. This technique has been extended to provide self-calibration of the ceiling, concurrent with HiBall tracking. Welch 2001 at Section 3.</p> <p>The original electro-optical tracker (figure 3, bottom) used independently housed lateral-effect photodiode units (LEPDs) attached to a lightweight tubular framework. As it turns out, the mechanical framework would flex (distort) during use, contributing to estimation errors. In part to address this problem, the HiBall sensor unit was designed as a single, rigid, hollow ball having dodecahedral symmetry, with lenses in the upper six faces and LEPDs on the insides of the opposing six lower faces (figure 7). This immediately gives six primary “camera” views uniformly spaced by 57 deg. The views efficiently share the same internal air space and are rigid with respect to each other. In addition, light entering any lens sufficiently off-axis can be seen by a neighboring LEPD, giving rise to five secondary views through the top or central lens, and three secondary views through the five other lenses. Overall, this provides 26 fields of view that are used to sense widely separated groups of LEDs in the environment. Although the extra views complicate the initialization of the Kalman filter as described in section 5.5, they turn out to be of great benefit during steady-state tracking by effectively increasing the overall HiBall field of view without sacrificing optical-sensor resolution.</p> <p>Welch 2001 at Section 4.1</p> <p>HiBall sensor unit was designed as a single, rigid, hollow ball having dodecahedral symmetry, with lenses in the upper six faces and LEPDs on the insides of the opposing six lower faces (figure 7). This immediately gives six primary “camera” views uniformly spaced by 57 deg. The views efficiently share the same internal air space and are rigid with respect to each other. In addition, light entering any lens sufficiently off-axis can be seen by a neighboring LEPD, giving rise to five secondary views through the top or central lens, and three secondary views through the five other lenses. Overall, this provides 26 fields of view that are used to sense widely separated groups of LEDs in the environment. Welch 2001 at Section 4.1.</p> <p>HiBall observes LEDs through multiple sensor-lens views that are distributed over a large solid angle. LEDs are sequentially flashed (one at a time) such that they are seen via a diverse set of views for each HiBall. Initial acquisition is performed using a brute-force search through LED space, but, once initial lock is made, the selection of LEDs to flash is tailored to the views of the active HiBall units. Pose estimates are maintained using a Kalman-filter-based prediction-correction approach known as single-constraint-at-a-time (SCAAT) tracking. This technique has been extended to provide self-calibration of the ceiling, concurrent with</p>

Exhibit E-6

CLAIM 8	Welch 2001
	<p>HiBall tracking. Welch 2001 at Section 3.</p> <p>At each estimation cycle, the next of the 26 possible views is chosen randomly. Four points corresponding to the corners of the LEPD sensor associated with that view are projected into the world using the 3x3x4 viewing matrix for that view, along with the current estimates of the HiBall pose. This projection, which is the inverse of the measurement relationship described above, results in four rays extending from the sensor into the world. The intersection of these rays and the approximate plane of the ceiling determines a 2-D bounding box on the ceiling, within which are the candidate LEDs for the current view. One of the candidate LEDs is then chosen in a least-recently-used fashion to ensure a diversity of constraints.</p> <p>Once a particular view and LED have been chosen in this fashion, the CIB (section 4.3) is instructed to flash the LED and take a measurement as described in section 5.2. This single measurement is compared with a prediction obtained using equation (3), and the difference (or residual) is used to update the filter state and covariance matrices using the Kalman gain matrix. The Kalman gain is computed as a combination of the current filter covariance, the measurement noise variance (section 6.2.1), and the Jacobian of the measurement model. This recursive prediction-correction cycle continues in an ongoing fashion, a single constraint at a time.</p> <p>Welch 2001 at Section 5.3.</p> <p>As a result of a mechanical design tradeoff, each sensor field of view is less than six degrees. The focal length is set by the size of the sensor housing, which is set by the diameter of the sensors themselves.</p> <p>Energetics is also a factor, limiting how small the lenses can be while maintaining sufficient light-collecting area. As a result of these design tradeoffs, even a momentary small error in the HiBall pose estimate can cause the recursive estimates to diverge and the system to lose lock after only a few LED sightings. And yet the system is quite robust. In practice, users can jump around, crawl on the floor, lean over, even wave their hands in front of the sensors, and the system does not lose lock. During one session, we were using the HiBall as a 3-D digitization probe, a Hi-Ball on the end of a pencil-shaped fiberglass wand (figure 14, left). We laid the probe down on a table at one point, and were amazed to later notice that it was still tracking, even though it was observing only three or four LEDs near the edge of the ceiling. We picked up the probe and continued using it, without it ever losing lock.</p>

Exhibit E-6

CLAIM 8	Welch 2001
	<div data-bbox="527 245 1142 532">  <p data-bbox="527 488 663 532">Figure 13.</p> </div> <div data-bbox="527 574 1520 1013">  <p data-bbox="527 954 663 998">Figure 14.</p> </div> <p data-bbox="512 1045 863 1084">Welch 2001 at Section 6.1.</p> <p data-bbox="512 1117 1967 1156"><i>See</i> Disclosures with respect to Claim 6, <i>supra</i>; <i>see also</i> Defendants' Invalidity Contentions for further discussion.</p>

G. DEPENDENT CLAIM 9

CLAIM 9	Welch 2001
[9] The method of claim 8 wherein the target	At least under Plaintiffs' apparent infringement theory, Welch 2001 discloses, either expressly or inherently, the method of claim 8 wherein the target comprises a natural feature in an environment. In the alternative, this element

Exhibit E-6

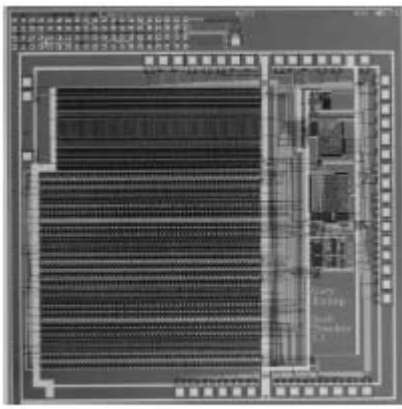
CLAIM 9	Welch 2001
<p>comprises a natural feature in an environment.</p>	<p>would be obvious over Welch 2001 in light of the other references disclosed in Defendants' Invalidity Contentions and/or the knowledge of one of ordinary skill in the art.</p> <p><i>See, e.g.:</i></p> <p>As part of his 1984 dissertation on Self-Tracker, Bishop put forward the idea of outward-looking tracking systems based on user-mounted sensors that estimate user pose by observing landmarks in the environment (Bishop, 1984). He described two kinds of landmarks: high signal-to-noise-ratio beacons such as light-emitting diodes (LEDs) and low signal-to-noise- ratio landmarks such as naturally occurring features. Bishop designed and demonstrated custom VLSI chips (figure 2) that combined image sensing and processing on a single chip (Bishop & Fuchs, 1984). The idea was to combine multiple instances of these chips into an outward-looking cluster that estimated cluster motion by observing natural features in the unmodified environment. Integrating the resulting motion to estimate pose is prone to accumulating error, so further development required a complementary system based on easily detectable landmarks (LEDs) at known locations.</p> <p>Welch 2001 at Section 1.2.</p> <div data-bbox="520 847 961 1334">  <p>Figure 2.</p> </div> <p>However, there are some significant advantages to the inside-looking-out approach for head tracking. By operating with sensors on the user rather than in the environment, the system can be scaled indefinitely. The</p>

Exhibit E-6

CLAIM 9	Welch 2001
	<p>system can evolve from using dense active landmarks to fewer, lower signal-to-noise ratio, passive, and some day natural features for a Self-Tracker that operates entirely without explicit landmark infrastructure (Bishop, 1984; Bishop & Fuchs, 1984; Welch, 1995).</p> <p>Welch 2001 at Section 2.</p> <p>Each HiBall observes LEDs through multiple sensor-lens views that are distributed over a large solid angle. LEDs are sequentially flashed (one at a time) such that they are seen via a diverse set of views for each HiBall. Initial acquisition is performed using a brute-force search through LED space, but, once initial lock is made, the selection of LEDs to flash is tailored to the views of the active HiBall units. Pose estimates are maintained using a Kalman-filter-based prediction-correction approach known as single-constraint-at-a-time (SCAAT) tracking. This technique has been extended to provide self-calibration of the ceiling, concurrent with HiBall tracking. Welch 2001 at Section 3.</p> <p><i>See</i> Disclosures with respect to Claim 8, <i>supra</i>; <i>see also</i> Defendants' Invalidity Contentions for further discussion.</p>